Surface chemical and physical modification in stent technology for the treatment of coronary artery disease

Feroze Nazneen, Grégoire Herzog, Damien W.M. Arrigan, Noel Caplice, Pasquale Benvenuto, Paul Galvin, Michael Thompson

▶ **To cite this version:**

HAL Id: hal-01829557

https://hal.univ-lorraine.fr/hal-01829557

Submitted on 8 Nov 2018

Surface chemical and physical modification in stent technology for the treatment of coronary artery disease

Feroze Nazneen[a], Grégoire Herzog[a#], Damien W.M. Arrigan[b], Noel Caplice[c], , Pasquale Benvenuto[d], Paul Galvin[a] and Michael Thompson[d]*

[a]*: Tyndall National Institute, Life Sciences Interface, University College Cork, Lee Maltings, Cork, Ireland*
[b]*: Nanochemistry Research Institute, Department of Chemistry, Curtin University, Perth, WA 6845, Australia*
[c]*: Biosciences Institute, Centre for Research in Vascular Biology, University College Cork, Cork, Ireland.*
[d]*: Department of Chemistry, University of Toronto, 80 St. George Street, Toronto, Ontario, Canada M5S 3H6*

* Corresponding author: E-mail: mikethom@chem.utoronto.ca

Abstract

Coronary artery disease kills millions of people every year. It results from a narrowing of the arteries (stenosis) supplying blood to the heart. This review discusses the merits and limitations of balloon angioplasty and stent implantation, the most common treatment options for coronary artery disease, and the pathophysiology associated with these treatments. The focus of the review is heavily placed on research efforts geared towards the modification of stent surfaces for the improvement of stent-vascular compatibility and the reduction in the occurrence of related pathophysiologies. Such modifications may be chemical or physical, both of which are surveyed here. Chemical modifications may be passive or active, while physical modification of stent surfaces can also provide suitable substrates to manipulate the responses of vascular cells (endothelial, smooth muscle, fibroblast). The influence of micro- and nano-structured surfaces on the *in vitro* cell response is discussed. Finally, future perspectives on the combination of chemical and physical modifications of stent surfaces are also presented.

[#]Present address: Laboratoire de Chimie Physique et Microbiologie pour l'Environnement, UMR 7564, CNRS, Nancy University, 405, rue de Vandoeuvre, F-54600 Villers-lès-Nancy, France

1. Introduction

Coronary artery disease (CAD) is the leading cause of death worldwide [1]. It results from the accumulation of fatty deposits within the arterial vessel wall which eventually leads to the narrowing, or "stenosis", of the arteries. The narrowing restricts blood flow and impedes the supply of oxygen and nutrients to the tissues. Health complications that may arise from CAD include clot formation, heart attack and stroke. The main risk factors for CAD at all ages, in both genders and in all geographical regions include hypertension, diabetes mellitus, smoking, obesity and cholesterol levels [2]. The first successful graft surgery involving a coronary artery bypass was performed in the 1960s for the treatment of CAD [3]. In this approach, arteries from elsewhere in the body of the patient were grafted to the coronary arteries to bypass the arterial stenosis resulting in improved blood supply to the heart muscle. However, this procedure possesses the disadvantage of clotting and subsequent stenosis of the vessel [4]. In 1977, Andreas Gruntzig pioneered balloon angioplasty, also called percutaneous transluminal coronary angioplasty. The technique involved passing a deflated balloon through a catheter to the vessel followed by inflation in order to open the artery and compress the plaque against the vessel wall [5]. In 1987, Sigwart introduced the first coronary stent, a medical device designed to serve as a temporary or permanent mechanical support within the artery [6]. Stents are meshed cylindrical scaffolds usually constructed from metals or polymers. The stent was typically inserted *via* a balloon catheter over a guide wire into a vascular lumen and expanded into contact with the diseased portion of the arterial wall, restoring adequate blood supply to the heart muscle. In addition to enlarging the lumen, balloon angioplasty causes some localized injury resulting in the initiation of restenosis of the artery at the angioplasty site. The process of restenosis involves inflammation, elastic recoil, thrombosis, neointimal proliferation and negative arterial remodeling [7-10]. When compared with balloon angioplasty, bare metal stents eliminate vessel elastic recoil and negative

remodeling [11] which significantly reduces the restenosis rate from 30-50 % to 20-30 %. This has been demonstrated by a number of landmark studies [12-13]. In spite of this achievement, neointimal hyperplasia (NIH), which results mainly from the over-proliferation of vascular smooth muscle cells (SMC) and the production of extracellular matrix components [11, 14], has remained the principle cause of in-stent restenosis.

The limitations exhibited by bare metal stents have led to the exploration of new stent materials, designs, surface treatments and coatings in order to improve the performance of the device, and in particular, attenuate the rate of in-stent restenosis. A major advance in the evolution of stents has been the use of drug-eluting stents (DES). DES have reduced the restenosis rate to 10% [15-17] by pharmaceutically inhibiting the proliferation of vascular SMC. Despite the decrease in the restenosis rate, DES have been criticized for hindering the natural healing process resulting from endothelial cell (EC) re-lining on and surrounding the stent struts. In addition, the use of DES has been associated with the risks of late stent thrombosis and needs longer-term dual antiplatelet therapy. Concern also remains regarding potential inflammation and hypersensitivity reactions caused by the polymer substrate of DES which may result in myocardial infarction and death [18-26]. A timeline summarizing the progress in the treatment of CAD is depicted in Figure 1. To circumvent the undesirable effects of permanent polymer-based metallic DES, polymer-free DES delivery systems and temporary biodegradable stents have been developed and evaluated. These new DES delivery systems have been produced to minimize the polymer burden and promote sustained drug-release rates.

Further improvement to stent technology is also being explored *via* micro- and nano-structured approaches on stent surfaces to manipulate vascular cell responses. The idea behind this strategy is to mimic the native structure of healthy endothelium or *in vivo* conditions, thereby reducing the potential for thrombosis and restenosis.

3

In the following sections, we review the current stent deployment techniques and stent types used for the treatment of CAD as well as the pathophysiology resulting from stent implantation. The various chemical modification strategies to improve stent-vascular compatibility are discussed and finally, the physical modification of surfaces to manipulate the vascular cell response is also described herein.

2. Current stent technology: Deployment techniques and types

Currently, over 100 types of stents are available in the marketplace primarily for vascular or non-vascular and peripheral indications [27]. Stents for coronary disease applications range from 2.0 to 4.0 mm in diameter and from 8 to 38 mm in length [28]. They are classified by deployment method (balloon-expandable or self-expanding) and by type (materials used, material forms, manufacturing methods and geometrical configurations). The required characteristics of current coronary stent materials and their delivery systems as described in other literature reviews are summarized in Table 1 [29-30].

In balloon-expandable stents, the stent is deployed by expanding it with a balloon catheter causing it to deform plastically. Stents of this type are fabricated with a smaller diameter and a low yield stress. By contrast, in the self-expanding deployment method, stents are manufactured with a diameter greater than that of the target vessel. The stent is constrained prior to deployment and then released to allow self-expansion. The material used for this deployment method must have a low elastic modulus and a high yield stress [31]. Comparative features of the balloon-expandable and self-expanding stents have been reviewed previously by Kathuria *et al* [32]. Studies have revealed that these modes of expansion vary with respect to late stent expansion and neointimal proliferation in stented lesions [33]. Common corrosion-resistant biomaterials employed for the manufacture of balloon-expandable bare-metal stents include 316L stainless steel, platinum-iridium (PtIr)

4

alloy, tantalum (Ta), cobalt-chromium (CoCr) alloy and titanium (Ti). Among these, 316L stainless steel is by far the most used alloy currently approved due to its excellent mechanical properties [34-35]. However, the biocompatibility of 316L steel is limited due to the instigation of thrombosis by the metal surface [36]. In addition, 316L steel is ferromagnetic and thus may interfere with magnetic resonance imaging protocols [37]. Despite these drawbacks, 316L stainless steel is often considered as a standard reference material for mechanical properties when developing new biomaterials for metallic stent applications. The other balloon-expandable metallic stents mentioned above are used for their improved radiopacity, superior radial strength, enhanced corrosion resistance, better magnetic resonance imaging compatibility, or the combination of all these characteristics. Among all these properties, improved radiopacity and superior radial strength are desired since they allow the design of stents with smaller delivery profiles. Nitinol is a nickel-titanium (NiTi) alloy that is widely used for producing self-expanding stents mainly because of its shape memory effects and super elasticity [38]. There is, however, a level of concern with this material associated with the possible release of Ni from the alloy which could lead to immunogenic reactions [38-39]. To address these concerns, surface passivation methods [40-42] and coatings [43-45] have been applied in order to enhance the Ti oxide concentration at the surface, thereby reducing the Ni concentration and improving the corrosion resistance.

For stent manufacture, three physical forms of materials are used: sheet, wire (round or flat) and tube. The selection of the stent fabrication method depends largely on the material form used. Currently, stents are produced largely by laser cutting, but also by other common methods that include electrode discharge machining, waterjet-cutting, photochemical etching from tubing, and various wire-forming techniques such as braiding and knitting [27, 32]. Geometry also plays an important role in the final mechanical properties of the stent. Early

designs classified the stent geometry into three basic types: slotted tube, coil and tubular mesh [27, 46]. Slotted tube stents are produced using tubes of metal from which a stent design is laser cut. Coil stents are made by metallic wires or strips formed into a circular coil shape, while tubular mesh stents consist of wires wound together in a meshwork forming a tube. A variety of stent geometrical designs can be further fashioned within a slotted tube, coil or tubular mesh framework. There are five basic types of stent configuration and these include coil, helical spiral, woven (braided or knitted), ring (individual or sequential) and cell (closed or opened) [27]. Figure 2 depicts the number of current FDA/CE-approved stent materials and their design types.. The stents differ slightly in strut pattern, width, length, diameter, interunit connections, geometry, flexibility, radial-strength, radiopacity, surface area coverage, metal content, metal composition and/or their delivery system [47]. These differing characteristics appear to profoundly influence both thrombosis and restenosis rates [48-50]. For example, studies have shown that stainless steel stents with tubular and corrugated designs are superior to coil or hybrid/mesh wire designs, and also to stents with rounded strut edges or thinner struts [51-55]. On the other hand, thinner struts appear more favorable than thicker struts in reducing the restenosis rates [56-60]. This suggests that stents with tubular, corrugated designs and thinner struts can be more effective in reducing the restenosis rate. Although metallic stent designs have improved the outcomes of patients undergoing percutaneous coronary intervention, the presence of permanent metallic stents has specific issues that limit their unrestricted use. These include chronic local inflammatory reactions, thrombogenicity, neointima formation, damaged endothelium, and mismatches in mechanical behavior between stented and non-stented tissues.

3. Pathophysiology related to stent deployment

The blood vessel wall, starting from the lumen of the vessel, consists of three layers: the intima, the media, and finally the adventitia. The layers are separated from each other by elastic fibers called the internal and external lamina. The luminal side of the intima is lined with ECs while the medial layer contains vascular SMC. The outer adventitial layer is composed of fibroblast cells (FC) and micro vascular networks. The properties of these three vascular cells play an essential role in the physiology of restenosis. Stent implantation causes physical damage to the vessel wall resulting in the stretching of the entire artery, endothelial denudation, and the compression and fracturing of the plaque. This damage also induces medial and, occasionally, adventitial dissection. In response to vessel wall injury, the body initiates a cascade of intravascular events leading to restenosis. Such events include inflammation, elastic recoil, NIH and arterial remodeling, and are each described below [11, 14, 61-62].

Inflammation within the vessel wall is observed after both balloon angioplasty and stent insertion and remains throughout all phases of restenosis. The inflammatory response is a localized protective reaction of tissues to injury.

Elastic recoil is due to contraction of the elastic fibers of the internal and external elastic laminae of the blood vessel wall in response to stretching and de-endothelialization. Recoil occurs within seconds to minutes after balloon deflation and results in the loss of up to 50% of the lumen gained after balloon inflation. As such, it defines the early phase of restenosis [63-64]. The rigid scaffolding provided by the stent significantly reduces elastic recoil, resulting in a larger initial gain in lumen size [12-13].

NIH occurs according to the following mechanism. Vessel injury caused by balloon angioplasty and stent deployment disrupts the endothelium, crushes the plaque and may induce medial dissection. Consequently, the sub-intimal components of collagen, fibronectin,

von Willebrand factor, and laminin become exposed. This results in the adherence, activation and aggregation of platelets, and the subsequent deposition of fibrin and thrombus formation. This is termed the thrombotic phase and can last hours to days [65-66]. The presence of an arterial wall injury, clot formation and a metallic foreign object attract circulating leukocytes and tissue macrophages. These de-marginate from the blood flow in what is called the recruitment phase, lasting 3 to 10 days [67-70]. The infiltration of these cellular elements stimulates the production of various growth factors and cytokines locally which in turn activate the vascular SMC [71-74]. Within the SMC, cyclin-dependent kinases and cyclins (regulators) drive the cell from one phase to another according to the following cycle: G_0, the resting phase; G_1, the growth phase; S, replication of DNA; G_2, preparation for division; and M, cell division. Collectively, they control the cell-cycle progression and therefore the reproduction of SMC [75-77]. The end result is the uncontrolled proliferation and migration of vascular SMC to the intima and stent lumen. The deposition of extracellular matrix by these cells eventually expands the neointimal layer within the stent lumen in what is called the neointimal proliferative phase. This phase may last weeks to months [78-79]. If the neointimal growth process is exuberant and significantly encroaches on the vascular lumen, then it will lead to in-stent restenosis. Stent deployment causes deeper vascular injury, more extensive thrombus formation and subsequently a greater degree of NIH than the original injury caused by balloon angioplasty [78-79]. DES have the important advantage of pharmaceutically inhibiting NIH, but they also impair re-endothelialization leading to delayed arterial healing and potential late stent thrombotic events [80].

Injury to the adventitial layer of the vessel wall results in **arterial remodeling** via FC proliferation, transformation to myofibroblasts, collagen synthesis, adventitial thickening, and increasing cell density [76]. This leads to a change in the artery wall size by constrictive re-modeling without a change in arterial wall mass. Remodeling occurs within weeks to months

after percutaneous coronary intervention [76]. Stenting eliminates the vascular remodeling by acting as a mechanical scaffold within the vessel [11, 81].

All these aforementioned events lead to restenosis, which is usually defined as a decrease in the luminal diameter of more than 50% at follow-up angiography. The restenosis rate is approximately 30-50% following balloon angioplasty [12]. This rate is reduced by an additional 20-30% [13] by bare metal stents, and further reduced by approximately 10% by DES [15-16]. However, despite advances in stent technology, the basic mechanism behind restenosis remains an area of highly active and ongoing research.

4. Chemical modifications to improve stent-vascular compatibility

Since stent technology fails to completely reduce sub-acute thrombosis and restenosis, systemic drugs (mainly anti-platelets and anti-thrombogenics) are administered in conjunction with stent implantation. *In vitro* data utilizing systemic drugs suggests that controlling mural thrombus formation may also reduce NIH. Dual anti-platelet therapy has greatly reduced the acute and sub-acute stent thrombosis rates. However, in clinical trials, systemic administrations of combinatory medicines have not demonstrated decreased restenosis rates [82-89].

The ineffectiveness of systemically administrated drugs may be due to their adverse effects and inadequate concentrations at the site of the stent implantation [90]. The limitations of these drugs have led to the development of stent surface modification approaches such as surface treatment and stent-coating systems. The former method is used mainly to obtain a clean and smooth surface texture for coronary stent material applications. The latter system is chiefly used as a platform for the facilitation of drug loading, while few stent coating materials are being used solely as a backbone material.

4.1 Stent surface treatments

Studies have shown that a rough surface is more prone to thrombogenicity [91-92] and thus surface treatments are essential to obtain a contamination-free and smooth surface for stent material applications. Various stent surface treatments include mechanical polishing, electropolishing, ultrasonic cleaning, chemical etching and degreasing as well as low-pressure plasma etching [93]. Electropolishing possesses several compelling advantages that render it the most popular surface treatment method [94]. Firstly, it can be performed on complex substrate shapes such as endovascular stents, leading to a well-passivated, smooth, defect- and contaminant-free surface. Secondly, it allows the removal of non-metallic inclusions and irregularities related to the initiation of various corrosion processes, especially localized corrosion. The electropolishing process features a metal that is anodically polarised in a suitable electrolyte solution together with a metal cathode [95]. Many parameters influence the electropolishing process. Such parameters include anodic current density, applied potential, bath temperature, polishing time, composition and concentration of electrolytes, agitation method and the anode-to-cathode surface area ratio (the geometry and gap between the two electrodes) [94]. Prior to electropolishing, acid pickling/descaling and annealing [96] are utilized to remove surface impurities such as debris, slags, scales, burrs and any other unwanted depositions caused by the laser cutting of the steel into a stent [97-98]. Some studies have reported that the polishing of coronary stent materials decreases clot and fibrinogen deposition [99] and may also reduce NIH in animal models [100-103]. To prevent the oxidation and deterioration of the stent product, surface passivation is performed after electropolishing [98]. This is followed by disinfection with isopropyl alcohol to prevent microbial contamination on the stent surface prior to drying with a hot air drier [98]. Surface smoothness and passivation of stents play important roles in reducing the restenosis rates. This needs to be taken into consideration in the development of new coating materials,

10

especially those for drug-elution applications as these coatings may have different surface roughnesses compared to bare metal stents.

4.2 Stent coatings

Device coating is an essential feature with respect to the design of stents since it affects both angiographic and clinical outcomes. Some materials exhibit superior mechanical properties but have unfavorable biocompatibilities, while other materials with better biocompatibility are not suitable for stent mass production because of unsuitable mechanical properties. The overall goal of stent coating thus involves combining the most desirable characteristics of different materials. From the literature [96], three main points have been highlighted for optimal stent coating. Firstly, it is necessary to perform the coating on a contamination-free metallic surface. Secondly, the surface roughness must be minimal compared to the film thickness to obtain good uniformity and adhesion of the film. Finally, the coating must be stable both when applied to the stent and during deployment.

The techniques commonly used for the production of stent coatings include galvanization [104], sputtering followed by ion bombardment [104], pulsed biased arc ion plating [105], dipping [106], spraying [107] and plasma-based depositions [108]. Coatings have been employed primarily to enhance stent biocompatibility, but recently they have also become a platform for the controlled delivery of drugs used to inhibit NIH [29]. Stent coatings can be broadly classified into passive and active coatings, both of which will be discussed further in the following subsections.

4.2.1. Passive coatings

Passive coatings act only as an inert barrier between the bloodstream/tissue and metal with good biocompatibility on a backbone material. Passive coatings are divided into inorganic and organic compounds, both of which are thought to be less thrombogenic and inflammatory, and

are thereby potentially able to reduce NIH [109]. Inorganic coating materials include metals, semiconductors, carbon compounds and ceramic coatings. Organic materials such as biostable, biodegradable and some biological polymers are utilized either as stent coatings or as vehicles for drug loading. Heparin, a biological coating, is applied as both a passive and active stent coating for drug-eluting platforms.

4.2.1.1 Inorganic stent coatings

Generally, inorganic coatings demonstrate a high degree of inertness (chemical stability), as well as good mechanical stability. This stability relegates them to mainly serve as passive hemocompatible coatings and corrosion inhibitors. The most commonly used inorganic coating materials for stents are metals such as gold (Au), chromium (Cr), titanium (Ti), platinum (Pt), and copper (Cu). Other inorganic stent materials include semiconductor silicon carbide (SiC), carbon compounds, and ceramic metal oxides [for example iridium-oxide (IrO) and titanium-nitride/oxide].

Gold is a chemically inert, radio-opaque, anti-corrosive material allowing facile stent deployment [90, 110-111]. Edelman *et al.* demonstrated that the thermal processing of Au coatings plays a significant role in neointimal proliferation in a pig model [112]. Human clinical trials, however, showed stent restenosis equivalency with uncoated stents [113-114], or enhanced neointimal formation compared with uncoated stents [57, 115-118]. Gold is no longer considered as a desired coating material due to its additional demonstrated thrombogenic nature.

Cr, Ti, Pt and Cu materials are known for their corrosion-resistant properties [111]. Ti reduces intimal growth, although this requires substantiation via clinical trials [104]. Pt and Cu induce prominent neointimal proliferation and stent thrombosis in animal models [104]. SiC is an amorphous, hydrogen rich semiconductor and may be less thrombogenic and inflammatory than bare metal stents [119-120]. *In vitro* studies on SiC-coated stents reported

a marked reduction in fibrin and thrombus formation [121]. Human studies with SiC-coated stents showed less acute thrombosis compared with bare metal stents [122], but reported no significant effect on NIH [123-125]. A diamond-like carbon coating is a chemically inert carbon-based material with improved biocompatibility [126]. Diamond-like carbon coated stents reported decreased NIH and restenosis in porcine arteries [127]. This study also showed that single layer diamond-like carbon coatings reduce NIH in a porcine model whereas two layers were not beneficial. Clinical trials in relatively high-risk patients showed that the "Carbostent™" (Sorin Medica, Italy), a metal stent coated with carbon, can significantly reduce stent thrombosis and restenosis [128]. However, these results were not supported by another study in terms of clinical outcomes [129].

IrO is a highly biocompatible inert ceramic material. A study in a porcine model showed that IrO stent coatings reduce neointimal thickness from 118µm to 55µm when compared to a bare metal stent [130]. A 316L stainless steel stent product called "Lunar™" (Inflow Dymanics, Munich, Germany) features a thin inner layer of gold for radiopacity and an outer layer of IrO for improved vascular compatibility (144). A clinical trial registry investigated the immediate and long-term effect of IrO coatings and reported that the overall angiographic restenosis rate was 13.8% [131]. This was attributed to the peroxide scavenging effect of the coating [131]. However, there is no clinical evidence to support its mechanism *in vivo* and there is an absence of randomized controlled clinical trials on this subject.

The titanium-nitride oxide (TiNOX) stent coating material acts as a barrier for metal ions and demonstrates high biocompatibility. Two types of titanium-nitride oxide stent coatings, TiNOX1 and TiNOX2, have been reported with ceramic and metallic properties. In an early porcine study, both titanium-nitride oxide stent coatings showed reduced in-stent thrombosis and neointimal proliferation [132]. In two clinical trials, titanium-nitride oxide coatings recorded angiographic restenosis rates of 15% and 33% with a reduction in major adverse

cardiac events (MACE) [133]. This coating has been demonstrated to be safe and effective even in unrestricted clinical studies that include high risks patients and complex lesions. Compared to DES, titanium-nitride oxide coated stents reported reduced MACE rates in long-term clinical trials [134-135]. The preponderance of data suggests that TiNOX stents have smaller MACE and target lesion revascularization event rates when compared to Taxus drug-eluting stents [135]. This appears to be one of the most promising coatings surveyed in this review, even despite the lack of a significant position in the marketplace.

4.2.1.2 Organic compounds

Organic polymers generally allow wider accessibility for chemical surface modification compared to inorganic substrates. Nevertheless, they are also more prone to alterations and hydrolytic degradation in the biological environment. A variety of biostable polymers, biodegradable polymers and biological materials are used as passive organic stent coatings. Biostable polymers possess good mechanical and biocompatible properties. Examples of biostable polymers include polyethylene terephthalate (PETP), expanded polytetrafluoroethylene (ePTFE), polyester (Dacron), a blend of polymethylmethacrylate (PMMA) and poly-2-hydroxyethyl methacrylate (PHEMA), fluorine-acryl-styrene-urethane-silicone (FASUS) copolymer, parylene, and amphiphilic polyurethane (PU). These materials reduce restenosis with varying degrees of success [29, 109, 136]. However, several polymer coatings have been associated with inflammation and increased neointimal formation in animal studies [136]. Nevertheless, the long-term outcome has not yet been assessed.

Biodegradable polymers have also shown good mechanical stability and sufficient blood compatibility. However, polymers such as polyglycolic acid (PGA)/polylactic acid (PLA), polycaprolactone (PCL), polyhydroxybutyrate valerate (PHBV), poly orthoester (POE) and polyethyleneoxide/polybutylene terephthalate (PEO/PBTP) demonstrated extensive inflammation and enhanced neointimal proliferation in a pig artery [137]. Recently, stents

14

coated with poly-(organophosphazene) (POPZ) and poly(L-lactic acid) (PLLA) [109, 136] exhibited less thrombogenesis, although their long-term effects have not yet been studied. Poly-bis-trifluoro-ethoxy phosphazene (PTFEP)-coated stents show good biocompatibility in a pig model for up to 6 months, offering surprisingly complete endothelial recovery at 5 days [136, 138]. Newly-developed poly (ester-amide) elastomers suggest that a slowly degrading material is suitable for stent-based local delivery in a porcine study [136, 139]. Consequently, biodegradable polymers with incorporated drugs have been developed (see section 4.2.2.3).

A variety of biocompatible polymers such as phosphorylcholine, hyaluronic acid, fibrin, and heparin are used as passive organic stent coatings. Biocompatible coatings must at least offer a surface that reduces undesirable tissue reactions, or preferably mimic a biological substrate that can facilitate healing around the site of stent implantation. Phosphorylcholine, hyaluronic acid, fibrin, and heparin are natural biological polymers extracted from plant and animal sources.

Phosphorylcholine is a neutral, zwitterionic, and naturally-occurring phospholipidic polymer [110]. It constitutes a vital part of the human red blood cell membrane. It is vaso-compatible, non-allergenic [29] and has drug-elution potential. The "BiodivYsio[TM]" stent (Biocompatibles Cardiovascular Inc., California, USA), which is coated with phosphorylcholine, was shown to be both safe and efficacious in the treatment of restenosis [140-142]. However, it did not provide better results than uncoated stainless steel stents in comparative clinical studies [143]. Hyaluronic acid is a linear polysaccharide, non-sulfated glycosaminoglycan component of the extracellular matrix. Administered hyaluronic acid and immobilized sulfated hyaluronic acid both cause decreased platelet aggregation and platelet adhesion in baboon models [144]. Although hyaluronic acid-coated stents appear promising as they were able to reduce thrombosis in baboon models [144], further studies of their efficacy in humans need to be conducted. Fibrin is an insoluble protein produced during

blood coagulation and is known for its biocompatible, biodegradable and viscoelastic properties [29, 145]. Exogenous fibrin coatings show less vessel occlusion and foreign body reaction than with PU and PETP polymers [146]. Fibrin-coated stents demonstrated complete endoluminal paving by covering 100% of the arterial surface, compared to the partial coverage attained with uncoated metal stents in a pig model [147]. Furthermore, fibrin may also facilitate rapid re-endothelialization. This coating strategy, while promising, requires testing in human trials to assess its full potential [148]. Heparin is a linear polysaccharide, sulfated glycosaminoglycan known for its anti-coagulant properties. Heparin has been evaluated mainly as a fixed passive stent coating, although it has also been studied as an active coating using a drug-eluting stent platform. Heparin-coated stents reported decreased rates of sub-acute thrombosis and reduced NIH relative to uncoated metal stents in animal studies [149-151]. In addition, stents coated with multiple layers of releasable heparin in porcine arteries showed less neointimal formation compared with bare metal stents [152]. However, human trials comparing heparin–coated to uncoated stents showed no significant impact on stent thrombosis and restenosis [153-155].

Despite such polymers aiding re-endothelialization and showing less inflammatory reactions in animal studies, human trials have not shown any significant differences from results obtained with bare metal stents.

4.2.2. Active stent coatings

Active coatings are usually based on the effect of therapeutic compounds which are either chemically bound directly to the surface of the stent, or trapped within a three-dimensional polymer that acts as a reservoir. Physicians have attempted to mitigate restenosis by administering drugs systemically, however most were ineffective in human trials despite promising preliminary work in animal models. The reason for the failure of this approach is

its inability to deliver a sufficient drug concentration at the site of injury. The current technology available for addressing the problem of concentration and averting restenosis is through the implantation of DES. These stents release one, or several bioactive agents into the blood and artery wall to reduce restenosis rates dramatically. DES can deliver higher concentrations of a drug locally without adverse systemic effects. DES can be divided into three main components: the stent, the pharmaceutically active compound, and a drug carrier (usually a polymer). The ideal DES should hinder thrombus formation, inflammation and cellular proliferation as well as enhance re-endothelialization [156]. The following topics for active stent coatings are discussed in the ensuing sub-sections: polymer-based, polymer-free and biodegradable DES, and healing-based approaches.

4.2.2.1. Polymer-based DES

Most of the pharmaceutical agents released by DES are blended with synthetic polymers that act as drug delivery vehicles which elute the active agent over time [90]. Unfortunately, many of these polymer-coated DES induce marked inflammatory and adverse responses in animal [90, 136, 157] and human subjects [26, 29, 158-160]. Additionally, polymer-based DES delay re-endothelialization and are considered as a significant factor in late stent thrombosis [21, 161] that can result in myocardial infarction and death [162]. Moreover, the incidence of stent related late thrombosis is reported to be higher in current polymer-based DES than bare metal stents, particularly after discontinuation of dual anti-platelet therapy [18-22, 26, 80]. Therefore, current research is focusing on biomimetic polymers such as phosphorylcholine and heparin (as mentioned in section 4.2.1.2), hydroxyapatite coatings (see section 4.2.2.2), novel biodegradable polymers, new stent materials (for specific lesions), and new drug combinations as well as biodegradable stents (described in section 4.2.2.3) to overcome the aforementioned problems of DES. Consequently, there is a need to develop devices for the delivery of drugs from stents using alternatives to the polymer-based vehicles. Thus, the

17

optimal composition of a DES in terms of the combination of the stent, active drug, and carrier has yet to be resolved in the development and management of CAD.

4.2.2.2 Polymer-free DES

Many alternative methods are under development for local delivery of drugs from stents without using permanent polymers or other carriers so as to avoid adverse responses from vascular ECs. Several of the non-polymer-based drug delivery technologies (porous platforms, strut micro-reservoirs, chemically-modified stents, magnetic nanoparticles and a stent free approach) that have been studied and reported in the literature for the treatment of CAD will be described here.

Porous coating materials that are currently being used for drug-loading include aluminum oxide, hydroxyapatite, carbon-carbon coatings and bare stainless steel stent surfaces. An aluminum oxide (Al_2O_3) stent coating is a highly biocompatible, inert ceramic material that can act as a vehicle for drug loading. Nanoporous surfaces have been produced by coating the stents first with a thin layer of aluminum by physical vapour deposition, with subsequent electrochemical conversion of aluminum to nanoporous Al_2O_3 [163]. A porcine study demonstrated that ceramic nanoporous Al_2O_3 coronary stent coatings (Yukon®, Jomed, Rangendingen, Germany), in combination with *Tacrolimus (an immunosuppressive drug)*, reduced both neointimal formation and the inflammatory response [163]. However, it was recently revealed that particle debris released from the nanoporous stent coating diminished the inhibitory effect of *Tacrolimus* [164]. Furthermore, clinical trials using this approach were not successful and this stent is currently not in use [165]. This technique is limited with regard to the drug-loading capacity and control over the drug-release kinetics. One study showed that uncontrolled release occurs when drugs adhere to the outer surface of the coating rather than being deposited within the pores [166]. Another study suggests that open porous

18

coatings may either require small pores to trap the drug for a longer period of time, or even a second coating to slow the rate of drug release [29].

Hydroxyapatite is a crystalline calcium phosphate. It is a biologically inert material and has also been used as a platform for drug delivery. In a study using pigs, nanoporous hydroxyapatite-coated stents (without drugs) exhibited a biocompatibility that was equivalent to that of uncoated stents [167]. A preliminary clinical trial of hydroxyapatite-coated stents loaded with anti-restenotic drugs showed promising results [168]. However substantial engineering challenges must be overcome in order to ensure durability and integrity of these ceramic coatings. This presents substantial challenges not only after deployment, but also during device construction, tracking through complex anatomy, and also when being positioned by direct stenting against hard lesions.

Microporous surfaces were created on stainless steel stents by a sandblasting technique. In porcine arteries, microporous stainless steel stents (Yukon[(R)] DES; Translumina, Hechingen, Germany) showed the ability to retain and release a drug over an extended period of time. This allows for dose adjustable, multiple and on-site coatings of drugs on metal stents [169]. Recent clinical trials demonstrated that this system was therapeutically effective when used in combination with *Rapamycin* (an immunosupressive drug) [170]. Although the clinical performance of sandblasted stents is encouraging, the on-site loading of drugs in clinics before stent insertion may introduce quality control issues.

Porous carbon-carbon coatings possess a glassy polymeric carbon matrix and pyrolytic carbon compounds. It appears that when the coating is initially in a polymer-based slurry with carbon particles dispersed, subsequent pyrolysis changes the mixture to the carbon-carbon matrix, with porosity controlled by the carbon particle size and the extent of pyrolysis. A preclinical evaluation using this drug-loaded coating on a CoCr stent showed the concept to be both safe and effective, although the study did lack a proper control experiment [171].

Further short- and long-term clinical trials using this technology are in progress. Reservoir surfaces have been produced by laser cut holes on stent struts and the holes were then loaded with drugs. However, the clinical effects of such stents (Carbostent[TM], Sorin Group, Italy) were not significantly different from control treatments [172]. In clinical trials, the direct attachment of the drug onto the stainless steel surface, without the use of polymers or any other drug delivery vehicles, showed no significant reduction in restenosis compared to bare metal stents [173]. A recent *in vitro* study demonstrated that a simple ethanol cleaning and heat treatment step after drug deposition improves the stability of the antiproliferative drug, *Paclitaxcel*, on Co-Cr alloys and allows the drugs to be delivered at a slower rate than un-cleaned and unheated samples [174].

In order to promote sustained drug release, drugs may also be chemically attached to metallic stent surfaces through the use of a self-assembled monolayer (SAM) intermediary. SAMs are single-layered molecular coatings that can be deposited on metal/metal oxide surfaces by the chemisorption of organic molecules from a contacting solution. Surface modification of biomaterials using SAMs has many potential biomedical applications. A range of biomolecules such as proteins [175-176], peptides [177-178], DNA [179-180], and antibodies [181-182] have been attached to SAMs. RGD peptides [183] and bone morphogenic proteins (BMP) [184] have also been tethered to SAMs to facilitate cell attachment on Ti surfaces. Recently, this technique has become a platform to coat and release therapeutic drugs directly from metal surfaces [185-187]. For instance, Mani *et al.* studied the interactions of human umbilical vein endothelial cells (HUVEC) with control, SAM and therapeutic SAM (TSAMs) coated Ti and Au specimens (TSAMs were SAMs derivatised with the drug, *Flufenamic acid*). This *in vitro* study demonstrated that SAMs and TSAMs do not elicit adverse reactions from HUVEC [187]. However, this approach needs to be verified in animal models and human subjects. Studies have shown that surface wettability,

roughness, charge, chemical composition and density of terminal functional groups are among the key factors that determine the adhesion and proliferation of cells on any material surface [187-188]. This should be taken into account when metal surfaces are coated with SAMs terminated with different functional groups, or when different varieties of therapeutic molecules are attached to SAMs for drug delivery applications. Although SAM coatings on Au [189-190] and Ti [183-184, 191-197] surface are well studied, the application of these strategies to coronary stents is very limited despite their widespread use in other biomedical applications. The formation of SAMs on key vascular stent materials such as 316L stainless steel [198-199], CoCr [200], NiTi [201-202] and Ta [203-204] is currently under investigation. In addition, an investigation of the long-term stability of SAMs on these stent materials is required. Although there are still some challenges to be overcome in the successful utility of polymer-free DES, these platforms do offer promising alternatives to the currently available polymer-coated DES.

Current DES platforms have limitations with respect to the adjustment of drug dose and release kinetics at the diseased arterial site. Maintaining constant therapeutic levels of drugs is not trivial a task. To address these challenges, local drug delivery mediated by stent targeted magnetic nanoparticles using uniform magnetic fields has been investigated. In a rat carotid artery study, enhanced retention of *Paclitaxel*-loaded biodegradable magnetic nanoparticles in the presence of a controlled and uniform magnetic field resulted in significant inhibition of SMC proliferation with a relatively low drug dose [205]. In addition, biodegradable magnetic nanoparticles were also used as a vehicle for loading both ECs and 304 stainless steel stents at the targeted site to promote artificial re-endothelialization and repeated dosing [206]. Although this approach seems effective, further preclinical and clinical trials are required as the strategy is still in the experimental stage.

4.2.2.3 Fully biodegradable stents

The problems of delayed re-endothelialization and late stent thrombosis that surround currently available permanent metallic DES are, in part, due to the presence of a foreign surface in contact with blood and tissue. This has stimulated research into biodegradable stents that could reduce the amount of exposure time, and thus the strain imposed on the body. Biodegradable stents provide temporary scaffolding to a narrowed arterial vessel followed by its disappearance once the vessel has healed. This approach may, in principle, reduce the risk of late stent thrombosis and thus can prevent subsequent coronary surgery. The technique may also lead to a reduction of problems associated with the obstruction of side-branches and concerns with overhang at ostial lesions [207-208]. Moreover, this device has the potential to deliver more drugs than the thin drug coatings on metallic stents. Two types of biomaterials have been explored as a basis for making biodegradable stents. The first are organic polymers, of which poly-L-lactic acid (PLLA) and tyrosine polycarbonate are the most widely used. The second are corrodible metals, predominantly either magnesium-based or iron-based alloys. Biodegradable stents that incorporate a variety of biodegradable polymer technologies that are either in development or in clinical trials are detailed in the following paragraphs.

A non-drug-eluting PLLA stent has demonstrated, in human trials, a low complication rate. However, concern has arisen about the ability to apply heat, in order to self-expand the stent, without causing possible thermal injury to the vessel wall [209]. As a result, these stents are not currently deployed in human coronaries. A biodegradable *Paclitaxel*-eluting coronary PLLA stent in long-term preclinical trials showed reduced proliferation and stenosis after vascular intervention [210]. However, studies with the *Everolimus*–eluting PLLA stent demonstrated reduced in-stent late loss and a low MACE rate of 4.4% at 9 months clinical outcomes with one non-Q wave myocardial infarction and one ischemia driven target lesion

revascularisation [211-212]. This indicates that there has been considerable improvement with respect to previous versions of the stent [213-214].

Acute recoil could be improved with a tyrosine polycarbonate stent, which possesses a 'slide and lock' design. In this case, a higher than anticipated target lesion revascularisation rate was observed at 4-6 months follow-up due to focal mechanical failures driven by polymer embrittlement. However, the degree of NIH was similar to that of bare metal stents [215-216]. The stent was redesigned resulting in the second-generation ReZolve™ stent (REVA Medical, San Diego, CA). This stent has a more robust polymer, a spiral 'slide and lock' mechanism to enhance clinical performance, and a coating of *Sirolimus*. Preclinical trials have been performed successfully and this stent is currently undergoing clinical evaluation [217]. Another biodegradable stent design combines an anti-proliferative drug with a polymer of salicylic acid to limit inflammation [218]. This stent demonstrated successful results in pig coronary arteries and in the case of human trials, reported absence of acute or chronic recoil. However, this stent showed insufficient neointimal inhibition due to inadequate drug dosing and very quick elution of *Sirolimus*. This issue has been addressed in a second generation stent through an optimized design and is currently under evaluation in pig and human coronaries [219-220]. One possible improvement that could be made to biodegradable salicylic acid stents would be to combine them with an anti- proliferative drug and endothelial progenitor cell capturing antibodies (section 4.2.2.4) to facilitate endothelialization.

There are few metals used in the production of biodegradable stents when compared with polymers. Biodegradable metal stents have been developed with the aim to provide superior mechanical strength, complete degradation and fast recovery of vasomotion compared to the polymer counterparts. For more detailed information on biodegradable metallic stents, the reader is referred to the review by Hermawan *et al.* [221]. So far, three generations of

magnesium stents have been introduced. The first generation AMS-1 stent, without any drug coating, showed a MACE of 26.7% at 12 months without deaths, stent thrombosis, or acute myocardial infarction in the PROGRESS-AMS trial [222]. A disappointing rate of target vessel revascularization [similar to the first generation REVA™ stent (REVA Medical, SanDiego, CA)] and in-stent late loss led to the development of a second generation, AMS-2 stent. This stent is characterized with prolonged degradation, a thinner strut thickness, and a modern design (modern designs have a square-shaped strut cross section instead of a rectangular shape in order to improve radial strength). In animal models, these changes have prolonged stent integrity and reduced neo-intimal proliferation [223]. Another version, the AMS-3 (drug-eluting AMS) stent, has been designed to reduce NIH. This version of the stent in animal trials reported a sustained release of an anti-proliferative drug at 28 days as compared to the AMS-1 stent [223]. Unlike magnesium stents, there has been little development with iron stents which remain in the pre-clinical phase. This may be partly due to the prolonged degradation times required and impending issues related with iron clearance. It appears at this point that fully biodegradable solutions to stenting hold the greatest promise, but longer-term studies are required to fully evaluate their safety and efficacy. At the time of this review, design of a safe DES still remains a challenge in the treatment of CAD.

4.2.2.4 Healing strategies

Damage to ECs and the intimal layer of the blood vessel wall is the basis for both thrombosis and NIH [29, 224]. Endothelialization of vascular stent surfaces is an alternative biological approach to stent design in which genetically engineered ECs are seeded on the stent prior to implantation to provide a protective natural covering which, in turn, inhibits thrombosis and NIH [225]. Van der Giessen *et al*. were the first to seed ECs on stents and study their *in vitro* behaviour. However, many *in vitro* attempts have reported narrowing of the arteries due to

the immediate loss of seeded cells, EC injury upon balloon expansion, and the inability to maintain cell adherence to the vessel wall under pulsatile flow [224-225]. To overcome the technical limitations of cell seeding, Bailey *et al.* [226] used local delivery of ECs after stent implantation in rabbit iliac and porcine arteries. After 4 h, both models displayed a greater number (>75%) of attached ECs on the implanted stents. By 14 days, EC coverage was >90% in both treated and untreated segments. Although these mature ECs contribute to the repair of endothelial injury, they have only limited regenerative capacity to do so. To circumvent this problem, as well as the risks associated with polymer-based DES, direct capture of endothelial progenitor cells (EPCs) (which have been identified as a source of reparative endothelium) from circulating blood was investigated. These are immature cells that are capable of differentiating into mature ECs. However, risk factors for CAD such as diabetes, hypercholesterolemia and hypertension are associated with impaired number and function of EPCs in these patients. To counteract this problem, studies have focused on the use of bioactive agents (so called "healing agents'') such as the CD34 antibody, vascular endothelial growth factors (VEGF), statins, hormones (estradiols), nitric-oxide donor compounds, and peptides to enhance re-endothelialization [227-236]. These healing agents are delivered locally *via* elution from coatings, surface-immobilizations, or through porous balloon catheters [227-236]. A novel approach to promoting the healing process has been through the use of the CD34 antibody-coated Genous[TM] stent (Orbus Neich, Fort Lauderdale, Florida) to capture circulating EPCs [237] . Results have shown that the Genous[TM] stent is effective in the reduction of restenosis [228, 238-240], but not to the same degree as commercially available DES. A similar, but still experimental concept, has been described by Blindt *et al.* who applied an RGD peptide coating to attract EPCs to the stent surface [241]. Another approach is the *Bevacizumab*-eluting phosphorylcholine stent (BiodivYsio[TM], Biocompatibles Cardiovascular Inc., California, USA) [242]. *Bevacizumab*, an antibody specific to VEGF,

25

was coated on the surface of BiodivYsio™ stents to inhibit the growth of *vasa vasorum*, and thereby promote atherosclerotic plaque stability.

Another alternative could be a technology that exploits a pro-healing strategy, such as an anti-CD34 coating on DES to improve re-endothelialization by attracting circulating EPCs, or applying drugs on the abluminal surface and therefore allowing re-endothelialization on the luminal surface [174, 243]. These newer technologies will have to undergo short- and long-terms safety trials to reveal their efficiency, both of which represent major obstacles.

5. Physical modification of stent surfaces for improved vascular cell function

Although currently available DES have reduced the probability of restenosis to 10 %, several drawbacks, as previously mentioned, remain and thus highlights the need for further improvements. This has generated research interest in the use of stent surface topography approaches for the control of vascular cell (EC, SMC, and FC) function. These three cell types play an important role in the healing process and maintenance of cardiovascular systems and are thus likely to be in contact with biomedical implants such as stents and grafts. Surface micro- and nano-structures may provide new solutions to the key remaining challenges though the control of these cells. Firstly, such structures could promote better vascular cell adhesion functioning through a complimentary mechanism to any of the systems described above. Secondly, they could decrease the need for systemic administration of drugs in a simple and cost effective manner. Finally, they could reduce the requirement for secondary surgery after stent implantation, thereby reducing chronic pain and stress.

Micro- and nano-topographies, independent of surface chemistry, have been shown to influence EC, SMC, and FC functions such as adhesion, alignment, morphology, proliferation, migration, and profiles of gene expression. Various topographical features such

as gratings, pits, posts, islands and random structures in micro- and nanoscale have been exposed to ECs (Table 2), SMC (Table 3) and FC (Table 4).

The effects of micro-topography on cellular functions have been previously studied and the methods for controlling them are well recognized [244]. Recently, nano-topographies have been receiving increasing interest because of their resemblance to the *in vivo* environment. However, the underlying mechanism behind the interaction between cells and nano-textured surfaces is still not well understood. It has been hypothesized that cells, *in vivo*, grow on a basement membrane composed of extracellular matrix proteins such as fibrous collagen, hyaluronic acid, proteoglycons, laminin and fibronectin [244]. In addition to its biochemical and mechanical properties, the basement membrane consists of nanometer size features in the form of pores, ridges or fibers [244]. These nanoscale features can be mimicked on biomaterial surfaces to promote the cellular functions desirable for biomedical implants, tissue engineering, regenerative medicine, cell-based sensors, and high through put arrays as well as to further our fundamental understanding of the very complex interactions between cells and synthetic surfaces. The key advances reported from studies on the response of ECs, SMC and FCs to surface micron, sub-micron and nano-topographies are discussed in the following sections. The specific micro- and nano-topographies that will be mentioned are gratings, pits, posts, islands (Figure 3) and random geometries.

5.1 Fabrication of artificial micro- and nano-structured surfaces

Recent advances in micro- and nanotechnology have allowed the patterning of surfaces with the necessary micro- and nano-structured features. Various techniques such as photolithography, focused-ion-beam lithography, e-beam lithography, nano-imprint lithography, interference lithography, reactive ion-etching, glancing angle deposition, physical vapor deposition, electrospinning, self-assembly patterning, colloidal lithography, polymer de-mixing, co-block phase separation and chemical etching or oxidation may be used to create 2D and 3D nano-structured features. These techniques have been described in detail elsewhere [245-248] and can yield uniform arrays of various features including gratings, posts, pits, and island geometries in the micro- and nanometer range. However, the aforementioned techniques each have their own merits and limitations which can vary with respect to material, geometry, cost and surface area coverage. Many micro- and nano-fabrication techniques are being developed. This is to create structured surfaces that arereproducible, reliable and can produce uniform arrays with fine features over a large surface area in a simple, fast and cost effective way, both on metal and polymeric biomaterials. In the literature, most *in vitro* studies have been conducted on 2D biological interfaces. Advanced fabrication techniques and biocompatible materials must be eventually synergized as a means to integrate cell nano-topographic interactions with advanced biomaterials. There are several advanced fabrication approaches for integrating nano-topographical cues into 3D structures. Two notable techniques include two-photon polymerization [249-250] and microscale origami [251-252]. Integration of nano-structures to 3D biomaterials and the generation of novel 3D structures remains a challenging pursuit.

5.2 Endothelial cell (EC) responses

Previous studies have reported that ECs could respond viably to surface topographical features in the micrometer, sub-micrometer and nanometer ranges summarized in Table 2. For example, Palmaz *et al.* [253] noticed that surface discontinuities at the microscopic scale influenced the conformation and motional dynamics of migrating ECs on NiTi surfaces. They also studied the effect of defined surface features on EC migration speed, long axis orientation, shape, size and density. It was concluded that these rates significantly increased (up to 64%) on surfaces with gratings ranging from 3 to 22 μm when compared to flat control surfaces. As a consequence of the increased migration rate, the ECs had a more elongated shape on the grating surfaces. These results were supported by a more recent study [254] in which stents with microscopic parallel gratings were placed in the carotid arteries of pigs. The authors reported that one week after implantation, stents with grated surfaces exhibited an endothelialization rate that was almost double that observed on stents with smooth surfaces. It was hypothesized that such patterns may reduce the time required for the endothelialization of vascular stents and thus reduces the risk of in-stent restenosis and late stent thrombosis. Other studies have proposed that since ECs align and elongate in the direction of blood flow *in vivo*, then the grating geometrical pattern may promote a similar trend. Lu *et al.*, for example, designed patterned Ti surfaces composed of periodic arrays of gratings with widths and spacings ranging from 750 nm to 100 µm using a plasma based dry-etch technique to study EC adhesion, proliferation and morphology. Their results demonstrated that ECs on nano-scale patterned Ti surfaces were oriented and displayed enhanced cell function as compared to smooth Ti surfaces, random nano-structured Ti surfaces and glass patterned surfaces [255]. In another study, Ashwini *et al.* reported enhanced EC adhesion and orientation on micro-patterned and nano-roughened poly

(dimethyl siloxane) (PDMS) films (compared to the un-patterned surfaces) that were fabricated using electron-beam evaporation of pure Ti and elastomer PDMS casting [256]. These studies reported that a line grating geometry induced the alignment and elongation of ECs that were similar to those encountered on native endothelium. In order to mimic the *in vivo* environment, Hwang *et al.* recently demonstrated a method for measuring the adhesion of human and calf ECs on nano-grating PLGA surfaces fabricated within a PDMS microfluidic channel using thermal imprinting and irreversible thermal bonding. The adhesion strength of ECs was measured by applying a range of shear stresses. Their results showed the greatest adhesion of ECs on nano-PLGA surfaces possessing 700 nm ridges and 350 nm gratings [257]. Bettinger *et al.* also showed increased EC adhesion and alignment, enhanced migration velocities and reduced proliferation on a nano-topographical surface with a line grating geometry. Moreover, this study also showed that cells form super-cellular-band structures that led to enhanced capillary tube formation on matrigel (extracellular matrix) substrates [258]. In short, many *in vitro* studies have reported that substrates with a grating pattern favor the adhesion, migration, alignment, and morphology of ECs. However, there have also been a number of reports describing reduced proliferation. This could be the result of either a surface chemical or topographical effect and requires further evaluation. Nevertheless, grating features created both on metallic and polymeric biomaterials demonstrated EC morphology and environments similar to the native endothelium. Therefore, grating geometries could be a useful therapeutic target for stent design and may enhance EC growth and healing.

The effect of nano-island geometry on EC behavior has also been investigated. For instance, Berry *et al.* reported decreased EC adhesion and spreading on nylon tubes with internal nano-topographies produced using polymer de-mixing [259]. Similarly, Hsu *et al.* showed that 27 nm islands created by diblock co-polymer de-mixing of PCL/poly (ethylene glycol) (PEG)

reduced EC spreading [260]. In contrast, Dalby *et al.* demonstrated enhanced EC spreading on 13 nm islands produced by polymer de-mixing of PS/poly bromostyrene (PBrS) as compared to cells grown on 35 nm and 95 nm islands, which in turn demonstrated increased EC spreading relative to that on flat control surfaces [261]. These studies highlight that slight changes in feature height produce large changes in EC behavior. In addition, surface chemistry may also have an effect on EC response because there is variation in the polymer mixtures and solvents employed for fabrication of the nano-structures. This result has been corroborated by Buttiglieri *et al.* [262] and Barbucci *et al.* [263]. Buttiglieri *et al.* also noticed a similar effect on a co-culture of ECs and leucocytes. ECs grown on all nano-island substrates adopted a curved/arcuate morphology [261] similar to that found in ECs that line the vasculature. Nevertheless, nano-geometrical islands have been shown to increase endocytotic activity [259]. In summary, these studies reveal that nano-island feature size and surface chemistry plays an essential role in EC adhesion and morphology and thus must be taken into consideration in the design of stent materials. However, this type of geometrical feature produced by polymer de-mixing applies to polymers only, while grating patterns can be created both on metallic and polymeric substrates.

A limited number of studies on the response of ECs to nano-posts have been reported. Of these studies, Kim *et al.* demonstrated that nano-post PEG surfaces fabricated using capillary lithography enhanced the focal adhesion of ECs *via* an increase in material surface area and adhesion sites for cells [264]. Recently, Zawislak *et al.* showed the development of ECs on 3D nano-post silicon surfaces with a depth of 10 µm, a periodicity of 6 µm and a diameter of 0.15 µm. In a sub-confluent layer, the cells impale themselves on the pillar to the extent that even some of the cell nuclei were penetrated by the pillar tips. In a confluent layer, the pillars were no longer detectable as the cells sat on top. This study found that inhibition of myosin-induced contractility caused the cells to relax around the pillars [265]. In summary, these

types of 2D and 3D topographical features seem to facilitate the adhesion of ECs. It is important to note that this feature type has only been fabricated on polymer substrates.

Some studies have been conducted on EC response to random topographies. For instance, Chaudhary *et al.* first demonstrated increased EC adhesion on Ti and CoCrMo vascular stent surfaces with random nano-structured features [266]. Recently, they have also reported enhanced EC function (including collagen and elastin synthesis) on nano-structured Ti compared to nano-smooth Ti [267]. In addition, Khang *et al.* demonstrated increased EC adhesion on nanometer and sub-micron rough Ti surfaces [268]. Similarly, Peng *et al.* showed significantly enhanced EC proliferation and secretion of (prostaglandins) PGI_2 on nano-tubular TiO_2 surfaces formed *via* anodic oxidation [269]. Samaroo *et al.* synthesised micron to nanometer-rough NiTi surfaces by using different constituent dimensions of NiTi powder. It was shown that ECs adhere and proliferate on NiTi surfaces with greater sub-micron and nanoscale roughness compared with coarse grain NiTi and conventional Ti surfaces [270]. Furthermore, Joseph *et al.* demonstrated increased EC adhesion on PLGA surfaces with vertical feature sizes of 0-19 nm due to an increase in surface free energy and subsequent serum protein (fibronectin and collagen type IV) adsorption [271]. These studies show that even a random nano-rough surface can influence EC behavior, which could be taken into consideration for stent designs and coating applications. However controlled feature dimensions, which is essential for reproducibility, cannot be obtained using this method,

It is interesting to note that even a simple chemical treatment can lead to nano-rough topographies. For example, Serrano *et al.* showed improved EC adhesion and proliferation on nano-rough poly (caprolactone) films (as compared to untreated samples) synthesised using sodium hydroxide (NaOH) etching [272]. In contrast, Miller *et al.* revealed decreased EC adhesion and proliferation on PLGA films with surface nano-topographies (compared to

micron-sized) created using NaOH etching [273]. This result has also been corroborated using nanometer-rough silica surfaces synthesized by colloidal silica nanoparticles [274]. These studies indicate the influence of various nanometer-rough surfaces in manipulating EC functions. Furthermore, variations in results were evident with different polymer materials even though the materials were treated with the same chemical. This implies that the selection of polymer and chemical treatment in creating random nano-structures plays a vital role on EC behavior.

Overall, of all the geometrical features described here, nano-grating topographies seem to promote significant EC adhesion, migration, alignment, and elongation. However reduced proliferation, when compared to other topographical features, has been demonstrated by *in vitro* studies. For example, nano-islands and nano-posts show increased proliferation. These studies highlight interesting observations about the feature size, feature geometry and surface chemistry effect on EC response. This approach may be useful for stent design that promotes healing of the vascular endothelium. However, this strategy is still under development and further *in vivo* studies are needed. No data on the influence of nano-pits on EC function have yet been reported. As such, further studies on nano-pits will be important.

5.3 Smooth muscle cell responses

Micro- and nano-grated topographies have been shown to influence the response of smooth muscle cells (SMC) on surfaces (Table 3). For instance, Sumona *et al.* reported that a micro-grated PDMS topography significantly enhanced the vascular SMC aspect ratio, alignment, and oriented remodeling of the extracellular matrix [275]. Glawe *et al.* reported high alignment of SMC on micro-fabricated PDMS surfaces created *via* layer by layer self-assembly of poly electrolytes. They found that the degree of alignment was channel-width dependent [276]. Houtchen *et al.* showed the influence of a combined cyclic strains and micro-gratings on the alignment and orientation of SMC [277]. Yim *et al.* showed significant

33

elongation, alignment, and reduced proliferation of SMC on PMMA and PDMS nano-patterned gratings produced by nano-imprint lithography [278]. The same authors also demonstrated that a nanostructured surface favoured the polarization of microtubule organizing centers in the direction of the cell alignment axis, whereas in the case of non-structured surfaces, microtubule organizing centers were polarized towards the wound edge. [278]. These studies showed that grating features can enhance the SMC alignment, elongation, and migration with a reduction of cell proliferation, similar to the effects on EC behavior. However, the studies of SMC on grating topographies were conducted on polymers and not on metal substrates. In this respect, it is important to again note that surface topography and material chemistry have an effect on cell behavior.

In a study by Richert $et\ al.,$ it was shown that there is no substantial influence of nano-pits in Ti_6Al_4V surfaces (produced by treatment with H_2SO_4/H_2O_2) on the growth of SMC [279]. In another study, Nguyen $et\ al.$ showed an unchanged response in SMC adhesion, an alteration in cell morphology and enhanced cell proliferation for cells grown on 200 nm pit surfaces compared to 20 nm pit surfaces. In addition, this study also reported that exposure of SMC to 200 nm pits induced the expression of various genes involved in cell cycle processes such as DNA replication, cell proliferation and signaling transduction pathways [280].

Multiple studies have investigated the response of SMC on random nano-topographies. For instance, Chaudhary $et\ al.$ demonstrated enhanced SMC adhesion and proliferation on random nano-structured metal stent surfaces compared to smooth surfaces [266]. Gao $et\ al.$ studied the effect of SMC in the presence of serum on nano-rough PGA fibers prepared by surface hydrolysis with NaOH. Their results demonstrated a significant increase in the density of SMC on surface-hydrolysed PGA fibers [281]. Increased bladder cell and vascular SMC adhesion and proliferation have also been reported on nano-structured casts of PLGA, PU and PCL films that were chemically treated with NaOH [272-273] or HNO_3 [282]. In

contrast, Peng *et al.* demonstrated decreased proliferation of SMC and increased expression of smooth α-actin on nanotubular TiO_2 surfaces [269].

As with ECs, grating topographies promoted SMC adhesion, alignment, elongation and decreased proliferation and decreased gene expression, whereas nano-pit and random topographies resulted in opposite effects. However, the influence of micro- and nano-gratings on the behaviour of SMC has only been examined for polymers

5.4 Fibroblast cell (FC) responses

FCs are widely studied as a model to investigate the influence of micro- and nano-grating island, pit and post geometries on cellular function (Table 4). Walboomer *et al.* studied FC adhesion, alignment, elongation and contact guidance on a variety of substrate materials with micro-grating topographies [283-286]. One investigation conducted by Meyle *et al.* found that while 100 % of FCs aligned to micro-gratings, alignment was observed for only 20% of macrophages and not at all in keratinocytes and neutrophils [287]. Lee *et al.* studied the influence of micro-grating dimensions on the behavior of FCs cultured on Ti substrates and revealed that micro-gratings of Ti with widths of 10 and 30 µm, as well as a depth of 3.5 µm, increased the cell viability, proliferation and up-regulation of fibronectin and integrin genes [288]. Similarly, human FCs elongated and aligned better on the micro-grated Ti substrates compared with the smooth Ti surfaces. The levels of fibronectin mRNA also increased as a result of the culture on the micro-grated surface [289]. In a different study, Biela *et al.* showed the FC response to grating patterns in the nanometer to micron range. Their results demonstrated stronger alignment, elongation and migration along the gratings of PDMS surfaces [290]. They also reported that a 50 nm grating depth induced the orientation response of FCs [290]. This result is in agreement with a study conducted by Loesberg *et al.* who showed that a lower threshold in grating depth (35 nm) induced the alignment and

orientation of FCs [291]. They also reported that gratings of depths less than 35 nm and widths less than 100 nm resulted in no cell alignment [291]. Similarly, Sun *et al.* studied the geometrical control of FCs on proton micro-machined 3D PMMA scaffolds. Their results indicated that wider and deeper gratings effectively retard the growth of FCs [292]. In brief, stronger alignment, elongation and migration of FCs were generally evident on grating topographies. This is similar to the results observed for ECs. These studies also point out the importance of feature depth, where FC growth was limited on wider and deeper grated features. This could be an important consideration in the development of stent designs.

Many studies have been conducted on FC response to nano-island geometry. Berry *et al.* demonstrated increased FC adhesion, spreading, morphology and cytoskeleton organization on nylon tubes exhibiting an internal nano-topography that was generated through polymer de-mixing [293]. Similarly, Dalby *et al.* reported a wide range of FC responses to nano-island topographies with heights of 10, 13, 27, 35, 45, 50, and 95 nm that were also created using polymer de-mixing [294-297]. The 10, 13 and 27 nm islands increased FC adhesion [294-295], proliferation, cytoskeletal development and up-regulation of gene expression [296-297]. Cell adhesion and proliferation on the 95 nm islands were reduced and the cells displayed the most stellate morphologies with poorly formed cytoskeletons [296]. Cells on the 35, 45, and 50 nm island surfaces had the same surface area as cells on flat controls, but with less developed cytoskeleton [295-296]. These studies highlight the fact that slight changes in feature height can produce very varied cellular responses. These experiments, however, did not reveal why the cells showed increased or reduced adhesion and growth on the different nano-islands. This type of surface structure created by polymer de-mixing is limited to polymers.

Some studies have investigated the response of FCs to nano-pits. One such study by Dalby *et al.* utilized arrays of nano-pits produced by e-beam lithography. Their results demonstrated

increased cell spreading and filapodia interactions on 120 nm pits when compared to 75 nm pits, while cells on 35 nm pits had a similar number of filopodia to those grown on control samples [298]. This group also demonstrated greatly decreased FC adhesion, spreading and broad transcriptional down regulation on PMMA substrates with nano-pits possessing a diameter of 120 nm, a depth of 100 nm and a pitch of 300 nm in a hexagonal arrangement produced by e-beam lithography [299]. These studies revealed that fibroblast cells prefer to grow on smaller sized features compared to larger ones. In a different study, Richert *et al.* demonstrated no significant influence on FC growth by nano-pit surfaces of Ti_6Al_4V created by oxidation with an H_2SO_4/H_2O_2 mixture [279]. This reiterates the importance of surface chemistry on cell behavior.

The effect of nano-post geometries on FC function was also investigated. Green *et al.* found that posts of 2 and 5 µm heights resulted in increased cell proliferation compared to 10 µm high posts and smooth surfaces. They also noted that the cells were attached to the post tops, which suggested that posts offer more mechanical interlocking units [300]. Kim *et al.* showed increased FC focal adhesion and growth on PEG nano-post surfaces fabricated using capillary lithography. They stated that the enhanced FC adhesion was due to increased material surface area [264]. In another study, Milner *et al.* observed FC adhesion and proliferation on PLA surfaces patterned with 400 nm and 700 nm posts *via* replication molding. Their results demonstrated increased FC adhesion and decreased cell proliferation on surfaces with 400 nm textures as compared to 700 nm textures and smooth surfaces. They proposed geometric constraints as a possible mechanism [301]. Furthermore, the same group showed that PLA topographic edge density and inter-topographic spacing enhanced FC adhesion [302]. In contrast, Hunt *et al.* demonstrated the effect of FC adhesion on polycarbonate and poly (etherimide) surfaces with micro-post features of varying dimensions that were generated by laser treatment. Their results demonstrated no FC orientation with respect to posts; FC spread

and elongate whether in contact with posts or microsmooth materials[303]. Similarly, Dalby *et al.* recently demonstrated reduced FC adhesion on PMMA substrates with nano-posts (prepared by colloidal lithography) that were 100 nm in diameter, 160 nm in height and having a pitch of 230 nm. An increase in endocytosis was also noted on nano-pits using clathrin staining indicating that these nano scale features are in the same size range as those features with which the *in vivo* cells interact with [304]. FCs have also been studied on silicon surfaces possessing nano-posts with a height ranging from 50-100 nm and with a pitch of 230 nm that were fabricated by interference lithography and deep reactive-ion etching [305]. Human FCs were found to attach in a similar density on flat control surfaces. However the cell morphology was more elongated on the nano-posts, an effect noticed for up to seven days in culture [306]. Scanning electron microscopy images of adhered FCs on these nano-post surfaces revealed that the cells conformed to the shape of the surface projection. Genes related to cytoskeletal formation and proliferation was found to be up-regulated. Cell cycle analysis of FC centromere positioning during interphase on nano-posts demonstrated that the centromeres were considerably closer together on the nano-posts compared to planar controls, which may impact cell proliferation [307-308]. In summary, nano-post geometries reviewed here showed reduced FC growth and increased gene expression.

FC behavior has also been investigated on random nano-rough geometries (Table 4). One *in vitro* study by Vance *et al.* showed decreased fibroblast numbers on NaOH-treated PLGA and PCL surfaces, as well as HNO_3-treated PU [309]. Cousins *et al.* have also shown that nano-rough surfaces created with silica nanoparticles affects FC morphology, decreases cell adhesion and inhibits cell spreading and thus cell proliferation for periods of up to seven weeks [310]. In brief, FC response to random nano-rough geometries created by chemical treatment showed no considerable effect on FC adhesion. These random geometrical features

can be applied for stent material design or drug delivery applications for the treatment of restenosis.

In general, stronger alignment, elongation, migration and decreased proliferation of FCs were reported on grated surfaces compared to island, post, pit and random topographies. The studies surveyed here also showed that feature depth, height and surface chemistry have a significant influence on cellular response. Lastly, it should be mentioned that nano-island and nano-post geometries were limited to polymers only.

5.5 Summary of studies on vascular cell responses to nano-structured surfaces

The formation of an EC lining on stent surfaces promotes healing of the vascular tissue, while SMC and FCs are mainly responsible for the restenosis of arteries. Therefore, the purpose of nano-structuring stent surfaces is to promote high EC adhesion, proliferation and migration and at the same time limit the adhesion, proliferation and migration of SMC and FCs. Such stent surfaces, which can selectively favour the growth of ECs over FCs and SMC could, in principle, reduce the risks of restenosis.

The shape and dimension of the nanostructures used on the stent surface play an important role on cell growth. In addition, nano-island and nano-post geometries are limited to polymeric materials whereas grating, pit and random features can be fabricated on both metallic and polymeric substrates. Gratings favor adhesion, alignment, elongation and migration and also reduce proliferation of all the vascular cells. Island structures on the substrate surface increases adhesion, proliferation, cytoskeleton organization and gene expression of ECs and FCs at dimensions of less than 27 nm whereas as above 27 nm, the same islands cause a decrease in these aforementioned cell responses. This highlights the importance of the feature height in promoting or reducing the growth of vascular cells. SMC

and FC responses reported on nano-pits decreased the growth and increased the proliferation, filopodia interaction and gene expression.

Materials used for the preparation of nanostructures can also impact cell behaviour. For example, an increase in the adhesion of ECs and FCs has been observed on nano-post PEG surfaces with depths of 300-500 nm, a pitch of 150 nm and a diameter of 50 nm, whereas a reduction in the adhesion and proliferation of FCs was noticed on nano-post surfaces of PMMA with depths of 100 nm, a pitch of 300 nm and a diameter of 120 nm. This could either be the result of the differences in material chemistry or nano-post dimensions, and thus requires further investigation. Enhanced EC and SMC adhesion and reduced FC adhesion were demonstrated on random topographies of PLGA and PCL surfaces. Similarly, enhanced EC adhesion and gene expression of SMC, but reduced proliferation of SMC was observed on nano-rough TiO_2 surfaces. However, the reproducibility of responses for all vascular cell types could be an issue with random topographies.

Vascular cell responses to micro- or nano-topographies rely on many factors such as cell type, feature size, feature geometry, and the physico-chemical properties of the substrate materials. No surface topography so far has been identified that promotes the adhesion of ECs over SMC and FCs. Future studies must be aimed at revealing the apparent reliance of the differential adhesion of vascular cells on feature dimension and geometry. Moreover, there are no widely accepted mechanisms for the effect of surface nano-topography on cell proliferation. Additional studies must be conducted to further examine the potential impact of nano-island, nano-post and nano-pit geometries on vascular cell migration profiles. No studies have been reported on the response of ECs to nano-pits and the influence of nano-posts and islands on SMC, so further studies on these strategies would be useful. Furthermore, studies must be conducted on nano-structured 316L stainless steel, CoCr and Ta vascular stent materials. To the best of our knowledge, no investigations have been reported

using these substrates which are commonly used for the fabrication of commercial stents. However, this does not appear to represent an ideal design as none of the *in vitro* topographic studies reported selective EC adhesion over SMC and FCs. Complementary approaches such as antibody-coated SAMs on nano-structured stent surfaces could facilitate the selective adhesion of circulating EPCs and promote endothelium healing. However, additional *in vitro* and *in vivo* studies must be conducted to assess the efficacy of this strategy.

6. Conclusion and future outlook

Over the past thirty years, improvements in percutaneous interventional approaches to CAD have led to a decrease in the restenosis rate to 10 %. In the evolution of this therapy, bare metal stents have been able to reduce the restenosis rate to 20% compared to balloon angioplasty by eliminating elastic recoil and negative arterial remodeling. However, bare metal stents are associated with a residual rate of sub-acute thrombosis and NIH. Variations in stent design have not demonstrated significant reductions in the restenosis rate, although tubular or corrugated designs, thinner struts, and electropolished stent surfaces have yielded better results in restraining NIH.

More attention has been paid to both chemical and physical modifications to the stent surface to further reduce the restenosis rate. Surface modifications have acted as a metal ion-barrier and as a delivery vehicle for drugs. Stents coated with passive elements did not significantly reduce restenosis compared to bare metal stents. However, passive inorganic stent coatings such as TiNOX and biological polymers including phosphorylcholine and hyaluronic acid coatings initially appeared promising, but long-term clinical trials will be necessary to determine the efficacy of these coatings.

Commercially available polymer-based DES have decreased in-stent restenosis but have also delayed re-endothelialization, raising concerns regarding late stent thrombosis, the need for

combinatory anti-platelet therapies, and polymer hypersensitivity. To address these concerns, biocompatible and biodegradable polymers were introduced, and subsequently, biodegradable polymeric and metallic stents were evaluated to avoid the late complications of bare metal stent implantation. The biodegradable polymer stents were constrained by mechanical strength and degradation issues, while the biodegradable metal stents appeared promising but lacked clear evidence of clinical superiority. Furthermore, the polymer-based problems have focused research attention back to bare metal stents and inorganic coatings in the field of polymer-free drug delivery vehicles or delivery of other biological and genetic agents.

An alternative strategy to stent design is to create biomimetic stent surfaces that could model the native structure of the healthy endothelium and hence promote faster healing of the vessel lumen after stent implantation. *In vitro* data suggests that micro- and nanoscale substrate topographies improve cell adhesion and migration but also reduce proliferation of vascular cells such as ECs, SMC and FCs. The ideal nano-structured substrate would facilitate re-endothelialization while inhibiting SMC and FC growth which are both responsible for restenosis. This might improve stent performance by eliminating the occurrence of in-stent restenosis. Such an approach could also be used in conjunction with current strategies that utilize bioactive agents or polymer-based drug delivery. However, this technology is still in the experimental phase. Another challenge that needs to be addressed is the engineering aspects related to the mass fabrication of such nano-structured stents. This approach will also need to be evaluated in preclinical and clinical studies.

7. Acknowledgements

Centre for Applied Nanotechnology, (a joint Enterprise Ireland and IDA Ireland initiative which was launched in 2007 as part of the Government's Strategy for Science Technology and Innovation (SSTI) 2006 -2013, PG); Science Foundation Ireland and Health Research Board (NC) and the Natural Sciences and Engineering Research Council of Canada (MT and PB).

Table 1: Desirable stent designs and their deployment characteristics

1. *Better Trackability* – ability to pass through tortuous vessels

2. *High expansion ratio* – the stent should undergo sufficient expansion and conform to the vessel wall

3. *Low profile* – ability to be crimped on the balloon catheter supported by a guide wire

4. *High scaffolding* – ability to provide strong mechanical support to the vessel wall

5. *Excellent corrosion resistance* – ability to prevent corrosion induced by formation of oxide films

6. *Good biocompatibility* – material must be biocompatible so as to not elicit an adverse reaction from the body

7. *Thrombo-resistivity* – the material should be blood compatible and not encourage platelet adhesion and deposition

8. *Adequate radiopacity/MRI compatibility* – to assist clinicians in assessing the *in vivo* location of the stent

9. *Inexpensive to manufacture* - –the stent material should be cost-effective to purchase

10. *Drug delivery* - the stent material should act as a vehicle for loading drugs

Table 2: Endothelial cell response to micro- and nano scale surface topographies

Feature geometry	Feature dimension	Fabrication technique	Materials	Endothelial cell response	Ref.
Grating	w:1, 3, 15, 22 µm		Ni-Ti	Alignment, elongation and enhanced migration	[253]
	w:750 nm - 100 µm; p: 750 nm, 2, 5, 75 and 100 µm	Plasma based dry-etching technique	Ti	Increased cell adhesion, alignment and elongation	[255]
	w: 20-80 µm d/h: 500 nm	e-beam, polymer casting	PDMS	Enhanced cell adhesion and elongation	[256]
	ridge w: 350, 700, 1050 nm; grating w: 350, 700, 1750 nm grating d/h: 500 nm	Thermal imprinting and irreversible channel bonding	PLGA	Highest adhesion on 700 nm ridges/350 nm grating	[257]
	w/d/h: 600 nm; p:1200 nm		PDMS	Alignment, elongation, enhanced migration and reduced proliferation. Also forms super-cellular- band structures	[258]
Islands	nm range	Polymer de-mixing	Nylon	Reduced adhesion, spreading. Increased endocytotic activity	[259]
	d/h: 27 nm	Polymer de-mixing	PCL/PEG	Reduced adhesion and spreading	[260]
	d/h: 13, 35, 95 nm	Polymer de-mixing	PS/PBrS	Increased adhesion, spreading, cytoskeleton re-organisation, gene up-regulation and exhibits arcuate morphology on 13nm	[261]
	d/h: 13- 95 nm	Polymer de-mixing	PS/PBrS and PnBMA /PS	Increased cell adhesion on 13 nm pits	[262]
	d/h: 18, 40, 95 nm	Polymer de-mixing	PS/PBrS	Increased cell adhesion on 18 nm	[263]
Post	dia: 50 nm ; d/h:300-500 nm; p:150 nm	Capillary lithography	PEG	Increased adhesion	[264]
	d/h: 10 µm; p: 6µm; dia: 0.15 µm	Laser irradiation and ablation	Silica	Increased cell monolayer formation	[265]

Random	nm range	Powder metallurgy, compact hydraulic press	Ti and CoCrMo	Increased cell adhesion and spreading	[266]
	nm range	Powder metallurgy, compact hydraulic press	Ti	Increased cell densities	[267]
	Sub-micron to nm	e-beam evaporator	Ti	Increased endothelial cell adhesion	[268]
	nm range	Anodic oxidation	TiO$_2$	Increased endothelial cell adhesion	[269]
	Sub-micron to nm		Ni-Ti	Increased adhesion and proliferation	[270]
	Sub-micron to nm	PS nanobeads and PDMS molds	PLGA	Increased endothelial cell adhesion	[271]
	nm range	NaOH etching	PCL	Increased endothelial cell adhesion and proliferation	[272]
	nm range	NaOH etching	PLGA	Decreased endothelial cell adhesion and proliferation	[273]
	nm range	Colloidal Silica solution	Silicon	Decreased endothelial adhesion, spreading and proliferation	[274]

w: width; dia: diameter; d: depth; h: height

46

Table 3: Smooth muscle cell response to surface topographies

Feature geometry	Feature dimension	Fabrication technique	Materials	Smooth muscle cell response	Ref.
Gratings	w/dia: 20, 50, 80 µm; d/p: 5 and 12 µm	Photolithography	PDMS	Enhanced smooth muscle cell aspect ratio, alignment, orientation remodeling of the underlying extracellular matrix	[275]
	w/dia: 10µm; d/h: 5 µm; p: 10 µm	Layer by layer assembly of polyelectrolytes	PDMS	Increased alignment and is grating width dependent	[276]
	w/dia: 15, 40 and 70µm; d/h: 5 µm; p: 14 µm	photolithography	PDMS	Combined micro topography and cyclic strains effect the orientation	[277]
	w/dia: 350 nm; d/h: 350 nm; p: 750 nm	Nano imprint lithography	PDMS, PMMA	Increased alignment, elongation, migration and reduced proliferation	[278]
Pits	d/h : 200 nm, 20 nm	Anodisation	Alumina	Enhanced proliferation and gene up regulation on 200 nm pits	[280]
	nm / µm range	H_2SO_4 / H_2O_2 etching	Ti6Al4V	No growth	[279]
Random	nm range	NaOH treatment	PGA	Increased adhesion and proliferation	[281]
	nm range	HNO_3 and NaOH etching and casting	PU, PLGA, PCL	Increased adhesion and proliferation	[282]
	nm range	NaOH etching and casting	PLGA	Increased cell densities	[273]
	nm range	NaOH etching	PCL	Increased cell adhesion	[272]
	nm range	Anodic oxidation	TiO_2	Decreased proliferation and increased expression of smooth muscle α-actin	[269]

w: width; dia: diameter; d: depth; h: height

Table 4: Fibroblast cell responses to surface topographies

Feature geometry	Feature dimension	Fabrication technique	Materials	Fibroblast cell response	Ref.
Gratings	w/dia: 1-10 µm; d/h : 1 µm; p: n/a	Photolithography and casting	PS	Orientation, alignment and spreading	[283]
	w/dia: 1-10 µm; d/h : 0.5 µm; p:n/a	Photolithography and casting, polymerization	PS, PLA, silicone, Ti coated PS	Induced contact guidance, cell morphology substrate dependant	[284]
	w/dia: 1-20 µm; d/h : 0.5-5.4 µm; p: n/a	Photolithography and casting	PS	Decreased adhesion, increased orientation on deeper grooves	[285]
	w/dia: 1-10 µm; d/h : 0.5 µm; p: n/a	Photolithography and casting	PS	Orientation on the narrow grooves and alignment groove depth dependant	[286]
	d/h: 0.5 µm; p: 1 µm	Photo lithography and anisotropic etching	Silicon dioxide	100% fibroblast alignment	[287]
	w/dia: 10, 30 µm; d: 3.5 µm; p: n/a	Micro-machining	Ti	Increased cell viability, proliferation and up regulation of fibronectin and integrin genes	[288]
	w/dia: n/a ; d/h: 3-5 µm; p: 6-10 µm	Micro-machining	Ti	Elongation, orientation and expression of fibronectin/mRNA	[289]
	w/dia: 2-10 µm; d/h: 50-200 nm; p: n/a	Photolithography	PDMS	Stronger fibroblasts alignment, elongation and migration	[290]
	w/dia: 20-1000 nm; d/h: 5-350 nm	e–beam, reactive ion etching	Silicon wafers	No adhesion and alignment below 35 nm	[291]
	w/dia: 266 nm; d/h: 5-530 nm; p: 1:1	Photolithography	Silicon	No alignment for depths < 35 nm or widths <100 nm	[291]
	µm range	Micro-machining	PMMA	No cell growth on wider and deeper gratings	[292]
Islands	nm range	Polymer de-mixing	Nylon	Increased adhesion, spreading, morphology and cytoskeleton organization	[293]
	w/dia: n/a; d/h: 95, 35, 27, 13 nm	Polymer de-mixing	PS/PBrS	Increased adhesion, spreading, cytoskeletion organization and gene up regulation on 13 and 27 nm pits. On 95 nm pits cells exhibits stellate morphology with	[296-297]

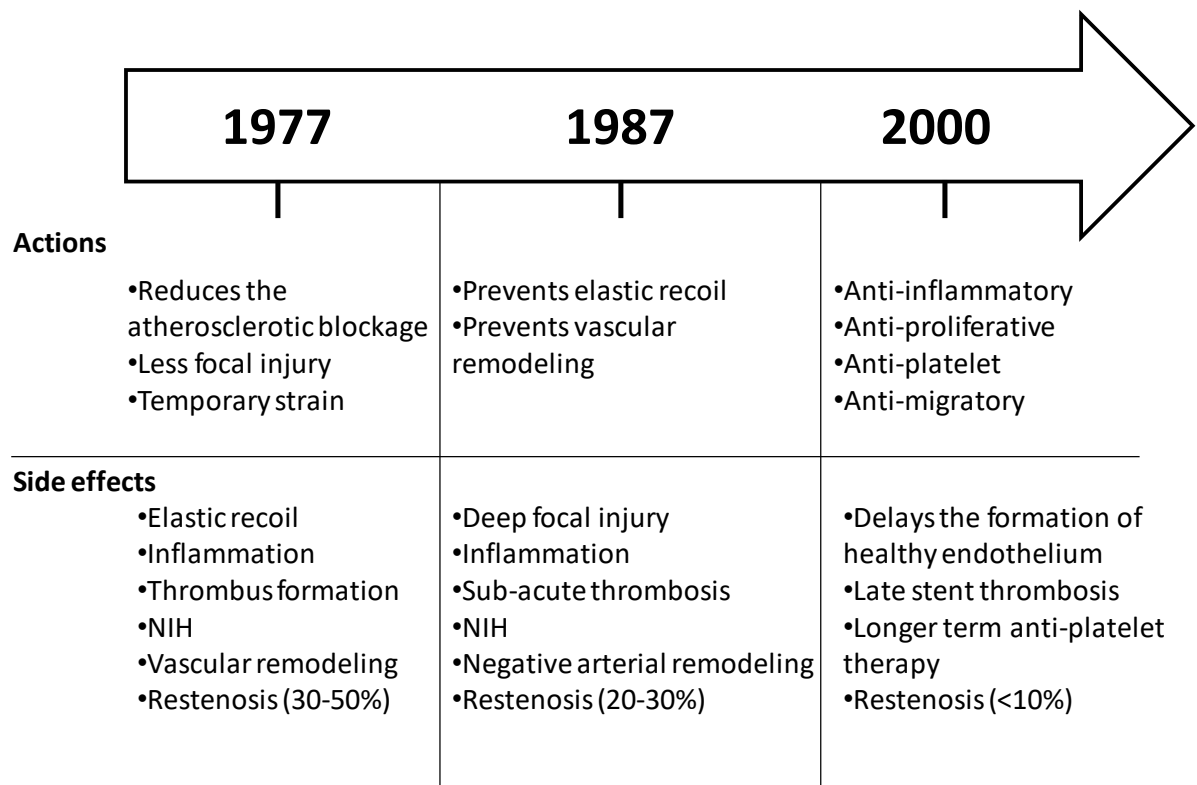|				less developed cytoskeleton	
	w/dia: n/a; d/h: 95, 45, 35, nm	Polymer de-mixing	PS/PBrS	Decreased adhesion and proliferation	[311]
	d/h: 10, 50 nm	Polymer de-mixing	PS/PBrS	10 nm pits showed increased cell adhesion, spreading and cytoskeletal reorganisation than the cells observed on 50 nm pits	[295]
Pits	dia: 35, 75, 120 nm; d/h: 50/100 nm	e-beam lithography	Silicon	Increased spreading and filopodia interaction on 120 nm than on 75 nm	[298]
	w/dia: 120 nm; d/h: 100; p: 300	e-beam lithography	PMMA	Smaller, less organized actin cytoskeleton. Less adhesion and spreading	[299]
	µm/nm range	Chemical treatment	TiAl$_6$V$_4$	No growth	[279]
Post	w/dia: 3 , 5, 10 µm	Photolithography	PDMS	3 and 5 µm showed better proliferation than the 10 µm post	[300]
	w/dia: 50 nm; d/h: 300-500 nm; p: 150 nm	Capillary lithography	PEG	Enhanced cell adhesion	[264]
	d/h: 400, 700 nm	Replication molding	PLA	Enhanced adhesion and decreased proliferation on 400 nm than on the 700 nm	[301]
	w/dia: 7, 25, 50 µm; d/h: 0.5, 1.5, 2.5 µm; p: 1:1	KrF laser	PC	No orientation and elongation	[303]
	w/dia: 100 nm; d/h:160 nm; p: 230	Colloidal lithography	PMMA	Reduced adhesion and increased endocytosis	[304]
	d/h: 50-100 nm; p: 230 nm	Interference lithography, deep reactive ion etching	Silicon	Increased elongation and alignment. Up regulation of genes.	[305-306]
Random	nm range	NaOH and HNO$_3$ treatment	PLGA, PCL, PU	Decreased adhesion and spreading	[309]
	7, 14 and 21 nm	Silica nano particles	Silica	Reduced adhesion and inhibits proliferation up to seven days	[310]

w: width; dia: diameter; d: depth; h: height

Figure Captions

Figure 1: Evolution in the treatment of restenosis from balloon angioplasty (I), to stent implantation (II) and drug-eluting stents (III).
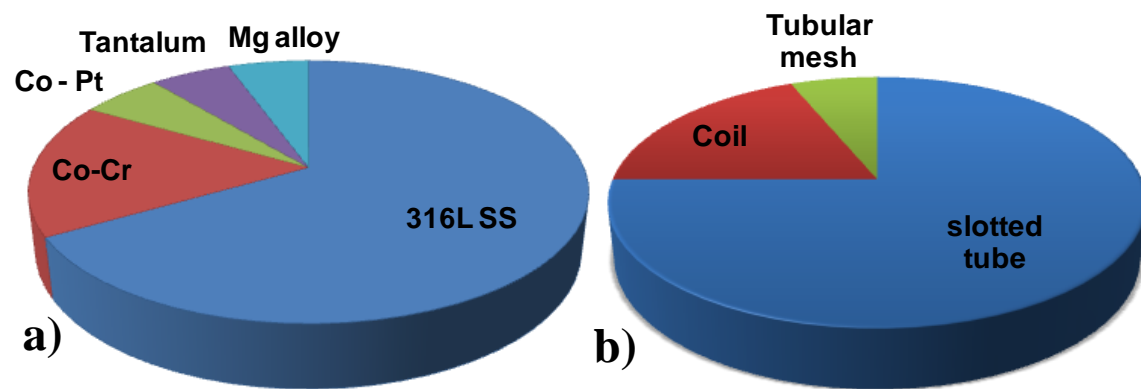
Figure 2: Repartition of FDA / CE approved stent materials (a) and design types (b).

Figure 3: Schematic depictions of nanotopography geometries. The four basic nanotopography geometries include a) nano-gratings, b) nano-post arrays, c) nano-pits, and d) nano-islands.
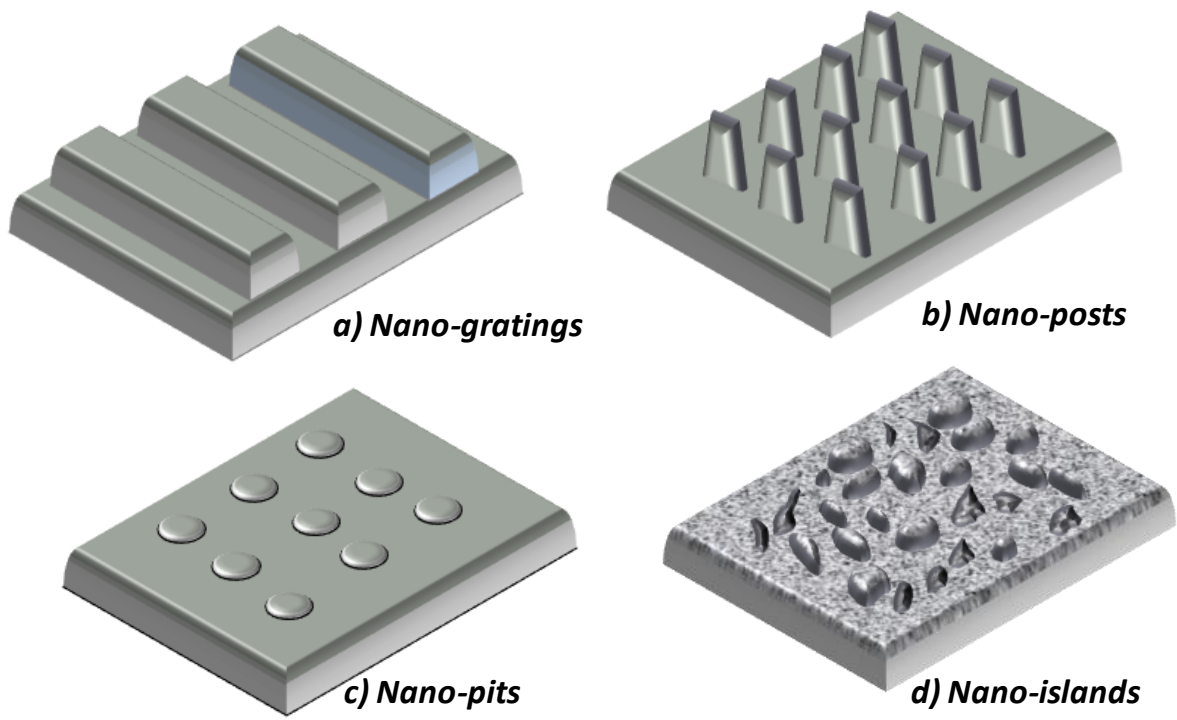
Figure 1

	1977	1987	2000
Actions	•Reduces the atherosclerotic blockage •Less focal injury •Temporary strain	•Prevents elastic recoil •Prevents vascular remodeling	•Anti-inflammatory •Anti-proliferative •Anti-platelet •Anti-migratory
Side effects	•Elastic recoil •Inflammation •Thrombus formation •NIH •Vascular remodeling •Restenosis (30-50%)	•Deep focal injury •Inflammation •Sub-acute thrombosis •NIH •Negative arterial remodeling •Restenosis (20-30%)	•Delays the formation of healthy endothelium •Late stent thrombosis •Longer term anti-platelet therapy •Restenosis (<10%)

Figure 2

Figure 3

a) Nano-gratings

b) Nano-posts

c) Nano-pits

d) Nano-islands

9. References

1.   Mackay J, Mensah G, The atlas of heart disease and stroke. Geneva. World Health Organization, 2004:84-91.
2.   Yusuf S, Hawken S, Ounpuu S, Dans T, Avezum A, Lanas F, McQueen M, Budaj A, Pais P, Varigos J, Liu LS, Investigators IS, Effect of potentially modifiable risk factors associated with myocardial infarction in 52 countries (the INTERHEART study): case-control study. Lancet, 2004;364:937-52.
3.   Haller JD, Olearchyk AS, Cardiology's 10 greatest discoveries. Tex. Heart Inst. J., 2002;29:342-4.
4.   Choi D, Hwang KC, Lee KY, Kim YH, Ischemic heart diseases: Current treatments and future. Journal of Controlled Release, 2009;140:194-202.
5.   Gruntzig A, Trans-Luminal Dilatation of Coronary-Artery Stenosis. Lancet, 1978;1:263.
6.   Sigwart U, Puel J, Mirkovitch V, Joffre F, Kappenberger L, Intravascular Stents to Prevent Occlusion and Restenosis after Trans-Luminal Angioplasty. N. Engl. J. Med., 1987;316:701-6.
7.   Klein LW, Rosenblum J, Restenosis after Successful Percutaneous Transluminal Coronary Angioplasty. Prog. Cardiovasc. Dis., 1990;32:365-82.
8.   Ip JH, Fuster V, Badimon L, Badimon J, Taubman MB, Chesebro JH, Syndromes of Accelerated Atherosclerosis - Role of Vascular Injury and Smooth-Muscle Cell-Proliferation. J. Am. Coll. Cardiol., 1990;15:1667-87.
9.   Rensing BJ, Hermans WRM, Beatt KJ, Laarman GJ, Suryapranata H, Vandenbrand M, Defeyter PJ, Serruys PW, Quantitative Angiographic Assessment of Elastic Recoil after Percutaneous Transluminal Coronary Angioplasty. Am. J. Cardiol., 1990;66:1039-44.
10.   Nobuyoshi M, Kimura T, Nosaka H, Mioka S, Ueno K, Yokoi H, Hamasaki N, Horiuchi H, Ohishi H, Restenosis after Successful Percutaneous Trans-Luminal Coronary Angioplasty - Serial Angiographic Follow-up of 229 Patients. J. Am. Coll. Cardiol., 1988;12:616-23.
11.   Lowe H, Oesterle SN, Khachigian LM, Coronary in-stent restenosis:Current status and future strategies. J. Am. Coll. Cardiol., 2002;39:183-93.
12.   Fischman DL, Leon MB, Baim DS, Schatz RA, Savage MP, Penn I, Detre K, Veltri L, Ricci D, Nobuyoshi M, Cleman M, Heuser R, Almond D, Teirstein PS, Fish RD, Colombo A, Brinker J, Moses J, Shaknovich A, Hirshfeld J, Bailey S, Ellis S, Rake R, Goldberg S, A Randomized Comparison of Coronary-Stent Placement and Balloon Angioplasty in the Treatment of Coronary-Artery Disease. N. Engl. J. Med., 1994;331:496-501.
13.   Serruys PW, Dejaegere P, Kiemeneij F, Macaya C, Rutsch W, Heyndrickx G, Emanuelsson H, Marco J, Legrand V, Materne P, Belardi J, Sigwart U, Colombo A, Goy JJ, Vandenheuvel P, Delcan J, Morel MA, A Comparison of Balloon-Expandable-Stent Implantation with Balloon Angioplasty in Patients with Coronary-Artery Disease. N. Engl. J. Med., 1994;331:489-95.
14.   Virmani R, Farb A, Pathology of in-stent restenosis. Curr. Opin. Lipidol., 1999;10:499-506.
15.   Morice M, Serruys PW, Sousa JE, Fajadet J, Hayashi EB, Perin M, Colombo A, Schuler G, Barragan P, Guagliumi G, Molnar F, Falotico R, A randomized comparison of a sirolimus-eluting stent with a standard stent for coronary revascularization. N. Engl. J. Med., 2002;346:1773-80.

16. Moses JW, Leon MB, Popma JJ, Fitzgerald PJ, Holmes DR, O'Shaughnessy C, Caputo RP, Kereiakes DJ, Williams DO, Teirstein PS, Jaeger JL, Kuntz RE, Sirolimus-eluting stents versus standard stents in patients with stenosis in a native coronary artery. N. Engl. J. Med., 2003;349:1315-23.

17. Grube E, Buellesfeld L, Initial experience with paclitaxel-coated stents. J. Interv. Cardiol., 2002;15:471-5.

18. Spertus JA, Kettelkamp R, Vance C, Decker C, Jones PG, Rumsfeld JS, Messenger JC, Khanal S, Peterson ED, Bach RG, Krumholz HM, Cohen DJ, Prevalence, predictors, and outcomes of premature discontinuation of thienopyridine therapy after drug-eluting stent placement results from the PREMIER registry. Circulation, 2006;113:2803-9.

19. Ong ATL, Serruys PW, in *Symposium of the Texas-Heart-Institute on Current Issues in Cardiology*, Texas Heart Inst, Orlando, FL, 2005, pp. 372-7.

20. McFadden EP, Stabile E, Regar E, Cheneau E, Ong ATL, Kinnaird T, Suddath WO, Weissman NJ, Torguson R, Kent KM, Pichard AD, Satler LF, Waksman R, Serruys PW, Late thrombosis in drug-eluting coronary stents after discontinuation of antiplatelet therapy. Lancet, 2004;364:1519-21.

21. Ong ATL, McFadden EP, Regar E, de Jaegere PPT, van Domburg RT, Serruys PW, Late angiographic stent thrombosis (LAST) events with drug-eluting stents. J. Am. Coll. Cardiol., 2005;45:2088-92.

22. Kuchulakanti PK, Chu WW, Torguson R, Ohlmann P, Rha SW, Clavijo LC, Kim SW, Bui A, Gevorkian N, Xue ZY, Smith K, Fournadjieva J, Suddath WO, Satler LF, Pichard AD, Kent KM, Waksman R, Correlates and long-term outcomes of angiographically proven stent thrombosis with sirolimus- and paclitaxel-eluting stents. Circulation, 2006;113:1108-13.

23. Iakovou I, Schmidt T, Bonizzoni E, Ge L, Sangiorgi GM, Stankovic G, Airoldi F, Chieffo A, Montorfano M, Carlino M, Michev I, Corvaja N, Briguori C, Gerckens U, Grube E, Colombo A, Incidence, predictors, and outcome of thrombosis after successful implantation of drug-eluting stents. JAMA-J. Am. Med. Assoc., 2005;293:2126-30.

24. Do drug-eluting stents increase deaths? , Retrieved September 11, 2006 from European Society of Cardiology, ESC Event News, 2006 World Congress of Cardiology. <http://www.escardio.org/vpo/News/events/wcc_drugelutingstents_events.htm>.

25. Boston scientific confirms long-term clotting risk of drug-eluting stents. Retrieved September 11, 2008 from Angioplasty.org website. <http://www.ptca.org/news/2006/0907.html>.

26. Nebeker JR, Virmani R, Bennett CL, Hoffman JM, Samore MH, Alvarez J, Davidson CJ, McKoy JM, Raisch DW, Whisenant BK, Yarnold PR, Belknap SM, West DP, Gage JE, Morse RE, Gligoric G, Davidson L, Feldman MD, in *54th Annual Scientific Session of the American-College-of-Cardiology*, Elsevier Science Inc, Orlando, FL, 2005, pp. 175-81.

27. Stoeckel D, Bonsignore C, Duda S, A survey of stent designs. Minim. Invasive Ther. Allied Technol., 2002;11:137-47.

28. Borovetz HS, Burke JF, Chang TMS, Colas A, Cranin AN, Curtis J, Gemmell CH, Griffith BP, Hallab NJ, Heller J, 2004, pp. 455–707.

29. Mani G, Feldman MD, Patel D, Agrawal CM, Coronary stents: A materials perspective. Biomaterials, 2007;28:1689-710.

30. Schatz RA, A view of vascular stents. Circulation, 1989;79:445-57.

31. Zahora J, Bezrouk A, Hanus J, Models of stents - Comparison and applications. Physiol. Res., 2007;56:S115-S21.

32. Kathuria YP, The potential of biocompatible metallic stents and preventing restenosis. Materials Science and Engineering a-Structural Materials Properties Microstructure and Processing, 2006;417:40-8.

33. Konig A, Schiele TM, Rieber J, Theisen K, Mudra H, Klauss V, Stent design-related coronary artery remodeling and patterns of neointima formation following self-expanding and balloon-expandable stent implantation. Catheter. Cardiovasc. Interv., 2002;56:478-86.

34. Park J, Bronzino J, *Biomaterials: principles and applications*, CRC press Boca Raton, FL, 2003.

35. Ratner B, *Biomaterials science: an introduction to materials in medicine, Second Edition*, Elsevier Academic press, 2004.

36. Thierry B, Merhi Y, Bilodeau L, Trepanier C, Tabrizian M, Nitinol versus stainless steel stents: acute thrombogenicity study in an ex vivo porcine model. Biomaterials, 2002;23:2997-3005.

37. Cardarelli F, in *Materials Handbook*, Springer London, 2008, pp. pp.59-157.

38. Shabalovskaya SA, On the nature of the biocompatibility and on medical applications of NiTi shape memory and superelastic alloys. Biomed. Mater. Eng., 1996;6:267-89.

39. BergerGorbet M, Broxup B, Rivard C, Yahia LH, Biocompatibility testing of NiTi screws using immunohistochemistry on sections containing metallic implants. J. Biomed. Mater. Res., 1996;32:243-8.

40. Maitz MF, Shevchenko N, Plasma-immersion ion-implanted nitinol surface with depressed nickel concentration for implants in blood. J. Biomed. Mater. Res. A, 2006;76A:356-65.

41. O'Brien B, Carroll WM, Kelly MJ, Passivation of nitinol wire for vascular implants - a demonstration of the benefits. Biomaterials, 2002;23:1739-48.

42. Trepanier C, Tabrizian M, Yahia L, Bilodeau L, Piron DL, Effect of modification of oxide layer on NiTi stent corrosion resistance. J. Biomed. Mater. Res., 1998;43:433-40.

43. Mazumder MM, De S, Trigwell S, Ali N, Mazumder MK, Mehta JL, Corrosion resistance of polyurethane-coated Nitinol cardiovascular stents. J. Biomater. Sci. Polym. Ed., 2003;14:1351-62.

44. Starosvetsky D, Gotman I, Corrosion behavior of titanium nitride coated Ni-Ti shape memory surgical alloy. Biomaterials, 2001;22:1853-9.

45. Shih CC, Lin SJ, Chung KH, Chen YL, Su YY, Increased corrosion resistance of stent materials by converting current surface film of polycrystalline oxide into amorphous oxide. J. Biomed. Mater. Res., 2000;52:323-32.

46. Butany J, Carmichael K, Leong SW, Collins MJ, Coronary artery stents: identification and evaluation. J. Clin. Pathol., 2005;58:795-804.

47. Burt HM, Hunter WL, Drug-eluting stents: A multidisciplinary success story. Adv. Drug Delivery Rev., 2006;58:350-7.

48. McLean D, Eiger N, Stent design: implications for restenosis. Rev. Cardiovasc. Med., 2002;3:S16.

49. Gurbel P, Callahan K, Malinin A, Serebruany V, Gillis J, Could stent design affect platelet activation? Results of the Platelet Activation in STenting (PAST) Study. J. Invasive Cardiol., 2002;14:584-9.

50. Kastrati A, Mehilli J, Dirschinger J, Pache J, Ulm K, Schühlen H, Seyfarth M, Schmitt C, Blasini R, Neumann F, Restenosis after coronary placement of various stent types. Am. J. Cardiol., 2001;87:34-9.

51. Yoshitomi Y, Kojima S, Yano M, Sugi T, Matsumoto Y, Saotome M, Tanaka K, Endo M, Kuramochi M, Does stent design affect probability of restenosis? A randomized trial comparing Multilink stents with GFX stents. Am. Heart J., 2001;142:445-51.

52. Rogers C, Edelman E, Endovascular stent design dictates experimental restenosis and thrombosis. Circulation, 1995;91:2995-3001.

53. Hausleiter J, Kastrati A, Mehilli J, Schuhlen H, Pache J, Dotzer F, Sattelberger U, Dirschinger J, Schomig A, Imp-act of lesion complexity on the capacity of a trial to detect differences in stent performance: Results from the ISAR-STEREO trial. Am. Heart J., 2003;146:882-6.

54. Lau K, Johan A, Sigwart U, Hung J, A stent is not just a stent: stent construction and design do matter in its clinical performance. Singapore Med. J., 2004;45:305-12.

55. Thuesen L, Andersen H, Krusell L, Botker H, Jorgensen E, Kelbaek H, Kristensen S, Randomized comparison of the coil-design Crossflex and the tubular NIR stent. Catheter. Cardiovasc. Interv., 2003;59:8-12.

56. Pache J, Kastrati A, Mehilli J, Schühlen H, Dotzer F, Hausleiter J, Fleckenstein M, Neumann F, Sattelberger U, Schmitt C, Intracoronary stenting and angiographic results: strut thickness effect on restenosis outcome (ISAR-STEREO-2) trial. J. Am. Coll. Cardiol., 2003;41:1283-8.

57. Hoffmann R, Mintz GS, Haager PK, Bozoglu T, Grube E, Gross M, Beythien C, Mudra H, vom Dahl J, Hanrath P, Relation of stent design and stent surface material to subsequent in-stent intimal hyperplasia in coronary arteries determined by intravascular ultrasound. Am. J. Cardiol., 2002;89:1360-4.

58. Briguori C, Sarais C, Pagnotta P, Liistro F, Montorfano M, Chieffo A, Sgura F, Corvaja N, Albiero R, Stankovic G, Toutoutzas C, Bonizzoni E, Di Mario C, Colombo A, In-stent restenosis in small coronary arteries - Impact of strut thickness. J. Am. Coll. Cardiol., 2002;40:403-9.

59. Kastrati A, Mehilli J, Dirschinger J, Dotzer F, Schuhlen H, Neumann F, Fleckenstein M, Pfafferott C, Seyfarth M, Schomig A, Intracoronary stenting and angiographic results: strut thickness effect on restenosis outcome (ISAR-STEREO) trial. Circulation, 2001;103:2816-21.

60. Pache J, Dibra A, Mehilli J, Dirschinger J, Schomig A, Kastrati A, Drug-eluting stents compared with thin-strut bare stents for the reduction of restenosis: a prospective, randomized trial. Eur. Heart J., 2005;26:1262-8.

61. Bennett MR, In-stent stenosis: pathology and implications for the development of drug eluting stents. Heart, 2003;89:218-24.

62. Karthikeyan G, Bhargava B, Prevention of restenosis after coronary angioplasty. Curr. Opin. Cardiol., 2004;19:500-9.

63. Rozenman Y, Gilon D, Welber S, Sapoznikov D, Gotsman MS, Clinical and Angiographic Predictors of Immediate Recoil after Successful Coronary Angioplasty and Relation to Late Restenosis. Am. J. Cardiol., 1993;72:1020-5.

64. Rodriguez AE, Palacios IF, Fernandez MA, Larribau M, Giraudo M, Ambrose JA, Time-Course and Mechanism of Early Luminal Diameter Loss after Percutaneous Transluminal Coronary Angioplasty. Am. J. Cardiol., 1995;76:1131-4.

65. White C, *Drug-Eluting Stents Advanced Applications for the Management of Coronary Disease.*, 2005.

66. Liu MW RG, King SB III Restenosis following coronary angioplasty potential biological determinants and role of intimal hyperplasia. Circulation, 1989;79:1374–87.

67.   Kornowski R, Hong MK, Tio FO, Bramwell O, Wu HS, Leon MB, In-stent restenosis: Contributions of inflammatory responses and arterial injury to neointimal hyperplasia. J. Am. Coll. Cardiol., 1998;31:224-30.

68.   Komatsu R, Ueda M, Naruko T, Kojima A, Becker AE, Neointimal tissue response at sites of coronary stenting in humans - Macroscopic, histological, and immunohistochemical analyses. Circulation, 1998;98:224-33.

69.   Ott I, Neumann FJ, Kenngott S, Gawaz M, Schomig A, Procoagulant inflammatory responses of monocytes after direct balloon angioplasty in acute myocardial infarction. Am. J. Cardiol., 1998;82:938-42.

70.   Smith-Norowitz TA, Shani J, Weiser W, Schulhoff N, Norowitz K, Lichstein E, Mokhtarian F, Lymphocyte activation in angina pectoris. Clin. Immunol., 1999;93:168-75.

71.   Breuss JM, Cejna M, Bergmeister H, Kadl A, Baumgartl G, Steurer S, Xu Z, Koshelnick Y, Lipp J, De Martin R, Losert U, Lammer J, Binder BR, Activation of nuclear factor-kappa B significantly contributes to lumen loss in a rabbit iliac artery balloon angioplasty model. Circulation, 2002;105:633-8.

72.   Cirillo P, Golino P, Ragni M, Battaglia C, Pacifico F, Formisano S, Buono C, Condorelli M, Activated platelets and leucocytes cooperatively stimulate smooth muscle cell proliferation and proto-oncogene expression via release of soluble growth factors. Cardiovasc. Res., 1999;43:210-8.

73.   Rectenwald JE, Moldawer LL, Huber TS, Seeger JM, Ozaki CK, Direct evidence for cytokine involvement in neointimal hyperplasia. Circulation, 2000;102:1697-702.

74.   Furukawa Y, Matsumori A, Ohashi N, Shioi T, Ono K, Harada A, Matsushima K, Sasayama S, Anti-monocyte chemoattractant protein-1 monocyte chemotactic and activating factor antibody inhibits neointimal hyperplasia in injured rat carotid arteries. Circ. Res., 1999;84:306-14.

75.   Schwartz R, Henry T, Pathophysiology of coronary artery restenosis. Rev. Cardiovasc. Med., 2002;3:S4.

76.   Salam AM, Al Suwaidi J, Holmes DR, Drug-eluting coronary stents. Curr. Probl. Cardiol., 2006;31:8-119.

77.   Clowes AW, Schwartz SM, Significance of Quiescent Smooth-Muscle Migration in the Injured Rat Carotid-Artery. Circ. Res., 1985;56:139-45.

78.   Schwartz RS, Henry TD, 2002, p. S4.

79.   Wong A, Chan C, Drug-eluting stents: The end of restenosis? Ann. Acad. Med. Singap., 2004;33:423-31.

80.   Joner M, Finn AV, Farb A, Mont EK, Kolodgie FD, Ladich E, Kutys R, Skorija K, Gold HK, Virmani R, Pathology of drug-eluting stents in humans - Delayed healing and late thrombotic risk. J. Am. Coll. Cardiol., 2006;48:193-202.

81.   Daemen J, Serruys PW, Drug-eluting stent update 2007 part I: a survey of current and future generation drug-eluting stents: meaningful advances or more of the same? Circulation, 2007;116:316-28.

82.   Unterberg C, Sandrock D, Nebendahl K, Buchwald AB, Reduced Acute Thrombus Formation Results in Decreased Neointimal Proliferation after Coronary Angioplasty. J. Am. Coll. Cardiol., 1995;26:1747-54.

83.   Schwartz RS, Holder DJ, Holmes DR, Veinot JP, Camrud AR, Jorgenson MA, Johnson RG, Neointimal thickening after severe coronary artery injury is limited by short-term administration of a factor Xa inhibitor - Results in a porcine model. Circulation, 1996;93:1542-8.

84.   Kastrati A, Schuhlen H, Hausleiter J, Walter H, ZitzmannRoth E, Hadamitzky M, Elezi S, Ulm K, Dirschinger J, Neumann FJ, Schomig A, Restenosis after coronary

stent placement and randomization to a 4-week combined antiplatelet or anticoagulant therapy - Six-month angiographic follow-up of the intracoronary stenting and antithrombotic regimen (ISAR) trial. Circulation, 1997;96:462-7.

85. Ellis S, Effron M, Gold H, Leon M, Popma J, Serruys P, Colombo A, Cohen N, Juran N, Werner W, Acute platelet inhibition with abciximab does not reduce in-stent restenosis (ERASER study). Circulation, 1999;100:799-806.

86. Tsuchikane E, Fukuhara A, Kobayashi T, Kirino M, Yamasaki K, Kobayashi T, Izumi M, Otsuji S, Tateyama H, Sakurai M, Awata N, Impact of cilostazol on restenosis after percutaneous coronary balloon angioplasty. Circulation, 1999;100:21-6.

87. Lee CW, Chae JK, Lim HY, Hong MK, Kim JJ, Park SW, Park SJ, Prospective randomized trial of corticosteroids for the prevention of restenosis after intracoronary stent implantation. Am. Heart J., 1999;138:60-3.

88. Meurice T, Bauters C, Hermant X, Codron V, VanBelle E, Mc Fadden EP, Lablanche JM, Bertrand ME, Amouyel P, Effect of ACE inhibitors on angiographic restenosis after coronary stenting (PARIS): a randomised, double-blind, placebo-controlled trial. Lancet, 2001;357:1321-4.

89. Serruys P, Foley D, Pieper M, Kleijne J, The TRAPIST Study. A multicentre randomized placebo controlled clinical trial of trapidil for prevention of restenosis after coronary stenting, measured by 3-D intravascular ultrasound. Eur. Heart J., 2001;22:1938.

90. Babapulle MN, Eisenberg MJ, Coated stents for the prevention of restenosis: Part I. Circulation, 2002;106:2734-40.

91. Depalma VA, Baier RE, Gott VL, Ford JW, Furuse A, Investigation of 3-surface properties of several metals and their relation to blood compatibility. J. Biomed. Mater. Res., 1972;6:37-75.

92. Hecker JF, Scandrett LA, Roughness and Thrombogenecity of the outer surfaces of intravascular catheters. J. Biomed. Mater. Res., 1985;19:381-95.

93. Trigwell S, Hayden RD, Nelson KF, Selvaduray G, Effects of surface treatment on the surface chemistry of NiTi alloy for biomedical applications. 1998;26:483-9.

94. Eliaz N, Nissan O, Innovative processes for electropolishing of medical devices made of stainless steels. J. Biomed. Mater. Res. A, 2007;83A:546-57.

95. William G.Wood AHC, ASM Surface Treating and Coating Division Council, American Chemical Society for metals, Ohio, 1982, p. 715.

96. Haidopoulos M, Turgeon S, Sarra-Bournet C, Laroche G, Mantovani D, Development of an optimized electrochemical process for subsequent coating of 316 stainless steel for stent applications. J. Mater. Sci. Mater. Med., 2006;17:647-57.

97. Zhao H, Van Humbeeck, J, Sohier, J, De Scheerder, I., Electrochemical polishing of 316L stainless steel slotted tube coronary stents. J. Mater. Sci. Mater. Med., 2002;13:911-6.

98. Raval A, Choubey A, Engineer C, Kothwala D, Development and assessment of 316LVM cardiovascular stents. Materials Science and Engineering a-Structural Materials Properties Microstructure and Processing, 2004;386:331-43.

99. Wang K, *Biocompatibilisation of coronary artery stents*, Leuven University Press, 1997.

100. Sheth S LF, Fishbein MC, Forrester JS, Eigler NL. , Reduced thrombogenicity of polished and unpolished nitinol vs. stainless steel slotted-tube stents in a pig coronary artery model. JACC, 1996:Abstracts-Poster:197A.

101. De Scheerder I, Verbeken E, Van Humbeeck J, Saunders, 1998, pp. 139-44.

102. De Scheerder I, Sohier J, Verbeken E, Froyen L, Van Humbeeck J, Biocompatibility of coronary stent materials: Effect of electrochemical polishing. Materialwissenschaft Und Werkstofftechnik, 2001;32:142-8.

103. De Scheerder I, Wang K, Sohier J, Verbeken E, Zhou XR, Frooyen L, Van Humbeeck J, Van de Werf F, Metallic surface treatment using electrochemical polishing decreases thrombogenicity and neointimal hyperplasia after coronary stent implantation in a porcine model. J. Am. Coll. Cardiol., 1998;31:277A-A.

104. Hehrlein C, Zimmermann M, Metz J, Ensinger W, Kubler W, Influence of Surface Texture and Charge on the Biocompatibility of Endovascular Stents. Coron. Artery Dis., 1995;6:581-6.

105. Liu CL, Chu PK, Lin GQ, Qi M, Anti-corrosion characteristics of nitride-coated AISI 316L stainless steel coronary stents. Surface & Coatings Technology, 2006;201:2802-6.

106. Heldman AW, Cheng L, Jenkins GM, Heller PF, Kim DW, Ware M, Nater C, Hruban RH, Rezai B, Abella BS, Bunge KE, Kinsella JL, Sollott SJ, Lakatta EG, Brinker JA, Hunter WL, Froehlich JP, Paclitaxel stent coating inhibits neointimal hyperplasia at 4 weeks in a porcine model of coronary restenosis. Circulation, 2001;103:2289-95.

107. Chen MC, Liang HF, Chiu YL, Chang Y, Wei HJ, Sung HW, A novel drug-eluting stent spray-coated with multi-layers of collagen and sirolimus. J. Control. Release, 2005;108:178-89.

108. Huang N, Leng Y, Yang P, Chen J, Sun H, Wang J, Wan G, Zhao A, Ding P, Surface modification of coronary artery stent by Ti-O/Ti-N complex film coating prepared with plasma immersion ion implantation and deposition. Nuclear Instruments and Methods in Physics Research Section B: Beam Interactions with Materials and Atoms, 2006;242:18-21.

109. Nguyen K, Su S, Zilberman M, Bohluli P, Frenkel P, Tang L, Eberhart R, Timmons R, Biomaterials and stent technology. Tissue engineering and novel delivery systems, 2004:p. 107.

110. Hara H, Nakamura M, Palmaz JC, Schwartz RS, Role of stent design and coatings on restenosis and thrombosis. Adv. Drug Delivery Rev., 2006;58:377-86.

111. Duda SH, Poerner TC, Wiesinger B, Rundback JH, Tepe G, Wiskirchen J, Haase KK, Drug-eluting stents: Potential applications for peripheral arterial occlusive disease. J. Vasc. Interv. Radiol., 2003;14:291-301.

112. Edelman E, Seifert P, Groothuis A, Morss A, Bornstein D, Rogers C, Gold-coated NIR stents in porcine coronary arteries. Circulation, 2001;103:429-34.

113. Harding S, McKenna C, Flapan A, Boon N, Long-term clinical safety and efficacy of NIROYAL vs. NIR intracoronary stent. Cathet. Cardiovasc. Diagn., 2001;54:141-5.

114. Cremonesi A, Benit E, Carlier M, Colombo A, Piva R, Probst P, Wirtzfeld A, Pico-Bourdonnec C, Corcos T, Multicenter registry to evaluate the efficacy of the NIROYAL™ Stent in de novo or restenotic coronary stenosis. J. Invasive Cardiol., 2000;12:225-35.

115. Kastrati A, Schomig A, Dirschinger J, Mehilli J, von Welser N, Pache J, Schuhlen H, Schilling T, Schmitt C, Neumann F, Increased risk of restenosis after placement of gold-coated stents: results of a randomized trial comparing gold-coated with uncoated steel stents in patients with coronary artery disease. Circulation, 2000;101:2478.

116. Hofma S, Van Beusekom H, Serruys P, van Der Giessen W, Recent Developments in Coated Stents. Current interventional cardiology reports, 2001;3:28.

117. vom Dahl J, Haager P, Grube E, Gross M, Beythien C, Kromer E, Cattelaens N, Hamm C, Hoffmann R, Reineke T, Effects of gold coating of coronary stents on

neointimal proliferation following stent implantation* 1. Am. J. Cardiol., 2002;89:801-5.

118. Danzi G, Capuano C, Sesana M, Di Blasi A, Predolini S, Antoniucci D, Patterns of in-stent restenosis after placement of NIR gold-coated stents in unselected patients. Catheter. Cardiovasc. Interv., 2002;55:157-62.

119. Monnink S, Van Boven A, Peels H, Tigchelaar I, De Kam P, Crijns H, Van Oeveren W, Silicon-carbide coated coronary stents have low platelet and leukocyte adhesion during platelet activation. Journal of investigative medicine: the official publication of the American Federation for Clinical Research, 1999;47:304-10.

120. Bolz A, Schaldach M, Artificial-Heart Valves - Improved Blood Compatibility by Pecvd a-Sic-H Coating. Artif. Organs, 1990;14:260-9.

121. Harder C, Rzany A, Schaldach M, Coating of vascular stents with antithrombogenic amorphous silicon carbide. Prog Biomed Res, 1999;4:71-7.

122. Heublein B, Pethig K, Elsayed A, Silicon Carbide Coating - A Semiconducting Hybrid Design of Coronary Stents - A Feasibility Study. J. Invasive Cardiol., 1998;10:255-62.

123. Kalnins U, Erglis A, Dinne I, Kumsars I, Jegere S, Clinical outcomes of silicon carbide coated stents in patients with coronary artery disease. Medical science monitor: international medical journal of experimental and clinical research, 2002;8:PI16-20.

124. Unverdorben M, Sippel B, Degenhardt R, Sattler K, Fries R, Abt B, Wagner E, Koehler H, Daemgen G, Scholz M, Comparison of a silicon carbide-coated stent versus a noncoated stent in human beings: The Tenax versus Nir Stent Study's long-term outcome. Am. Heart J., 2003;145:17-.

125. Tanajura L, Abizaid A, Feres F, Pinto I, Mattos L, Staico R, Randomized intravascular ultrasound comparison between patients that underwent amorphous hydrogenated Silicon-Carbide coated stent deployment versus uncoated stents (abstr.). J. Am. Coll. Cardiol., 2003;41:58A.

126. Gutensohn K, Beythien C, Bau J, Fenner T, Grewe P, Koester R, Padmanaban K, Kuehnl P, In vitro analyses of diamond-like carbon coated stents: Reduction of metal ion release, platelet activation, and thrombogenicity. Thromb. Res., 2000;99:577-85.

127. Airoldi F, Colombo A, Tavano D, Stankovic G, Klugmann S, Paolillo V, Bonizzoni E, Briguori C, Carlino M, Montorfano M, Comparison of diamond-like carbon-coated stents versus uncoated stainless steel stents in coronary artery disease. Am. J. Cardiol., 2004;93:474-7.

128. Antoniucci D, Valenti R, Migliorini A, Moschi G, Trapani M, Bolognese L, Santoro G, Cerisano G, Clinical and angiographic outcomes following elective implantation of the Carbostent in patients at high risk of restenosis and target vessel failure. Cathet. Cardiovasc. Diagn., 2001;54:420-6.

129. Colombo A, Airoldi F, Passive Coating: The Dream Does Not Come True. J Invas Cardiol, 2003;15:566-7.

130. Seliger C, McCall R, Wolf WP, Resch A, Alt EU, Influence of a rough, ceramic-like stent surface made of iridium oxide on neointimal structure and thickening in an animal study: 1 and 6 month data. Circulation, 2000;102:733.

131. Di Mario C, Grube E, Nisanci Y, Reifart N, Colombo A, Rodermann J, Muller R, Umman S, Liistro F, Montorfano M, Alt E, MOONLIGHT: a controlled registry of an iridium oxide-coated stent with angiographic follow-up. Int. J. Cardiol., 2004;95:329-31.

132. Windecker S, Mayer I, De Pasquale G, Maier W, Dirsch O, De Groot P, Wu YP, Noll G, Leskosek B, Meier B, Hess OM, Working Grp Novel Surface C, Stent coating with

titanium-nitride-oxide for reduction of neointimal hyperplasia. Circulation, 2001;104:928-33.

133. Windecker S, Simon RD, Lins M, Klauss V, Eberli FR, Roffi M, Pedrazzini G, Moccetti T, Wenaweser P, Togni M, Tuller D, Zbinden R, Seiler C, Mehilli J, Kastrati A, Meier B, Hess OM, Randomized comparison of a titanium-nitride-oxide coated stent with a stainless steel Stent for coronary revascularization. Circulation, 2005;111:2617-22.

134. Karjalainen P, Ylitalo A, Niemelä M, Kervinen K, Mäkikallio T, Pietilä M, Sia J, Tuomainen P, Nyman K, Airaksinen K, Two-year follow-up after percutaneous coronary intervention with titanium-nitride-oxide-coated stents versus paclitaxel-eluting stents in acute myocardial infarction. Annals of medicine, 2009;41:599-607.

135. Karjalainen PP, Annala AP, Ylitalo A, Vahlberg T, Airaksinen KEJ, Long-term clinical outcome with titanium-nitride-oxide-coated stents and paclitaxel-eluting stents for coronary revascularization in an unselected population. Int. J. Cardiol., 2010;144:42-6.

136. Kraitzer A, Kloog Y, Zilberman M, Approaches for prevention of restenosis. J. Biomed. Mater. Res. B Appl. Biomater., 2008;85B:583-603.

137. van der Giessen W, Lincoff A, Schwartz R, van Beusekom H, Serruys P, Holmes D, Ellis S, Topol E, Marked inflammatory sequelae to implantation of biodegradable and nonbiodegradable polymers in porcine coronary arteries. Circulation, 1996;94:1690-7.

138. Shikanov A, Vaisman B, Krasko MY, Nyska A, Domb AJ, Poly(sebacic acid-co-ricinoleic acid) biodegradable carrier for paclitaxel: In vitro release and in vivo toxicity. J. Biomed. Mater. Res. A, 2004;69A:47-54.

139. Lee SH, Szinai I, Carpenter K, Katsarava R, Jokhadze G, Chu CC, Huang YM, Verbeken E, Bramwell O, De Scheerder I, Hong MK, In-vivo biocompatibility evaluation of stents coated with a new biodegradable elastomeric and functional polymer. Coron. Artery Dis., 2002;13:237-41.

140. Grenadier E, Roguin A, Hertz I, Peled B, Boulos M, Nikolsky E, Amikam S, Kerner A, Cohen S, Beyar R, Stenting very small coronary narrowings (< 2 mm) using the biocompatible phosphorylcholine-coated coronary stent. Catheter. Cardiovasc. Interv., 2002;55:303-8.

141. Galli M, Bartorelli A, Bedogni F, DeCesare N, Klugmann S, Maiello T, Miccoli F, Moccetti T, Onofri M, Paolillo V, Pirisi R, Presbitero T, Sganzerla P, Viecca M, Zerboni S, Lanteri G, Italian BiodivYsio open registry (BiodivYsio PC-coated stent): Study of clinical outcomes of the implant of a PC-coated coronary stent. J. Invasive Cardiol., 2000;12:452-8.

142. Zheng H, Barragan P, Corcos T, Simeoni J, Favereau X, Roquebert P, Guerin Y, Sainsous J, Clinical experience with a new biocompatible phosphorylcholine-coated coronary stent. J Invasive Cardiol, 1999;11:608-14.

143. Moses J, Buller C, Nukta E, Aluka A, Barbeau G, Popma J, Moussa I, New G, Fiet F, The first clinical trial comparing a coated versus a non-coated coronary stent: The Biocompatibles BiodivYsio™ stent in randomised control trial (distinct). Circulation, 2000;102:11664.

144. Verheye S, Markou CP, Salame MY, Wan B, King SB, Robinson KA, Chronos NAF, Hanson SR, Reduced thrombus formation by hyaluronic acid coating of endovascular devices. Atherioscler Thromb Vasc Biol, 2000;20:1168-72.

145. Radosevich M, Goubran HA, Burnouf T, Fibrin sealant: Scientific rationale, production methods, properties, and current clinical use. Vox Sang., 1997;72:133-43.

146. Holmes DR, Camrud AR, Jorgenson MA, Edwards WD, Schwartz RS, Polymeric Stenting in the Porcine Coronary-Artery Model - Differential Outcome of Exogenous

Fibrin Sleeves Versus Polyurethane-Coated Stents. J. Am. Coll. Cardiol., 1994;24:525-31.

147. McKenna CJ, Camrud AR, Sangiorgi G, Kwon HM, Edwards WD, Holmes DR, Schwartz RS, Fibrin-film stenting in a porcine coronary injury model: Efficacy and safety compared with uncoated stents. J. Am. Coll. Cardiol., 1998;31:1434-8.

148. Byer A, Peters S, Settepani F, Pagliaro M, Galletti G, Fibrin sealant coated stents compared with non-coated stents in a porcine carotid artery model - Preliminary study report. J. Cardiovasc. Surg. (Torino), 2001;42:543-9.

149. DeScheerder I, Wang K, Wilczek K, Meuleman D, VanAmsterdam R, Vogel G, Piessens J, VandeWerf F, Experimental study of thrombogenicity and foreign body reaction induced by heparin-coated coronary stents. Circulation, 1997;95:1549-53.

150. Hardhammar PA, vanBeusekom HMM, Emanuelsson HU, Hofma SH, Albertsson PA, Verdouw PD, Boersma E, Serruys PW, vanderGiessen WJ, Reduction in thrombotic events with heparin-coated Palmaz-Schatz stents in normal porcine coronary arteries. Circulation, 1996;93:423-30.

151. Ahn YK, Jeong MH, Kim JW, Kim SH, Cho JH, Cho JG, Park CS, Juhng SW, Park JC, Kang JC, Preventive effects of the heparin-coated stent on restenosis in the porcine model. Catheter. Cardiovasc. Interv., 1999;48:324-30.

152. Matsumoto Y, Shimokawa H, Morishige K, Eto Y, Takeshita A, Reduction in neointimal formation with a stent coated with multiple layers of releasable heparin in porcine coronary arteries. J. Cardiovasc. Pharmacol., 2002;39:513-22.

153. Semiz E, Ermis C, Yalçinkaya S, Sancaktar O, Deger N, Comparison of initial efficacy and long-term follow-up of heparin-coated Jostent with conventional NIR stent. Jpn. Heart J., 2003;44:889-98.

154. Haude M, Konorza T, Kalnins U, Erglis A, Saunamaki K, Glogar H, Grube E, Gil R, Serra A, Richardt H, Heparin-coated stent placement for the treatment of stenoses in small coronary arteries of symptomatic patients. Circulation, 2003;107:1265-70.

155. Wohrle J, Al-Khayer E, Grotzinger U, Schindler C, Kochs M, Hombach V, Hoher M, Comparison of the heparin coated vs the uncoated Jostent (R) - no influence on restenosis or clinical outcome. Eur. Heart J., 2001;22:1808-16.

156. Pendyala L, Jabara R, Shinke T, Chronos N, Robinson K, Li J, Hou D, Drug-Eluting Stents: Present and Future. Cardiovasc. Hematol. Agents Med. Chem., 2008;6:105-15.

157. Nguyen K, Su SH, Zilberman M, Bohluli P, Frenkel P, Tang L, Eberhart R, Timmons R, Tissue engineering and novel delivery systems, 2004, p. 107.

158. Virmani R, Guagliumi G, Farb A, Musumeci G, Grieco N, Motta T, Mihalcsik L, Tespili M, Valsecchi O, Kolodgie FD, Localized hypersensitivity and late coronary thrombosis secondary to a sirolimus-eluting stent should we be cautious? Circulation, 2004;109:701-5.

159. Virmani R, Farb A, Guagliumi G, Kolodgie FD, Drug-eluting stents: caution and concerns for long-term outcome. Coron. Artery Dis., 2004;15:313-8.

160. Virmani R, Kolodgie F, Farb A, Drug-eluting stents: Are they really safe? Am. Heart Hosp. J., 2004;2:85-8.

161. Finn AV, Nakazawa G, Joner M, Kolodgie FD, Mont EK, Gold HK, Virmani R, Vascular responses to drug eluting stents. Arterioscler. Thromb. Vasc. Biol., 2007;27:1500-10.

162. Harper RW, Drug-eluting coronary stents - a note of caution. Med. J. Aust., 2007;186:253-5.

163. Wieneke H, Dirsch O, Sawitowski T, Gu YL, Brauer H, Dahmen U, Fischer A, Wnendt S, Erbel R, Synergistic effects of a novel nanoporous stent coating and

tacrolimus on intima proliferation in rabbits. Catheter. Cardiovasc. Interv., 2003;60:399-407.

164. Kollum M, Farb A, Schreiber R, Terfera K, Arab A, Geist A, Haberstroh J, Wnendt S, Virmani R, Hehrlein C, Particle debris from a nanoporous stent coating obscures potential antiproliferative effects of tacrolimus-eluting stents in a porcine model of restenosis. Catheter. Cardiovasc. Interv., 2005;64:85-90.

165. Tsujino I, Ako J, Honda Y, Fitzgerald PJ, Drug delivery via nano-, micro and macroporous coronary stent surfaces. Expert Opin. Drug Deliv., 2007;4:287-95.

166. Kang H, Kim D, Park S, Yoo J, Ryu Y, Controlled drug release using nanoporous anodic aluminum oxide on stent. Thin solid films, 2007;515:5184-7.

167. Rajtar A KG, Yang Q, Hakimi D, Liu D, Tsui M, Lien M, Smith D, Clubb FJ, Troczynski T., Hydroxyapatite-coated cardiovascular stents. EuroIntervention, 2006;2:113-5.

168. Costa JR, Abizaid A, Costa R, Feres F, Tanajura LF, Mattos LA, Staico R, Siqueira D, Sousa A, Bonan R, Sousa JE, Preliminary Results of the Hydroxyapatite Nonpolymer-Based Sirolimus-Eluting Stent for the Treatment of Single De Novo Coronary Lesions A First-in-Human Analysis of a Third-Generation Drug-Eluting Stent System. Jacc-Cardiovascular Interventions, 2008;1:545-51.

169. Wessely R, Hausleiter J, Michaelis C, Jaschke B, Vogeser M, Milz S, Behnisch B, Schratzenstaller T, Renke-Gluszko M, Stover M, Inhibition of neointima formation by a novel drug-eluting stent system that allows for dose-adjustable, multiple, and on-site stent coating. Arterioscler. Thromb. Vasc. Biol., 2005;25:748-53.

170. Mehilli J, Kastrati A, Wessely R, Dibra A, Hausleiter J, Jaschke B, Dirschinger J, Schomig A, Randomized trial of a nonpolymer-based rapamycin-eluting stent versus a polymer-based paclitaxel-eluting stent for the reduction of late lumen loss. Circulation, 2006;113:273-9.

171. Bhargava B, Reddy NK, Karthikeyan G, Raju R, Mishra S, Singh S, Waksman R, Virmani R, Somaraju B, A novel paclitaxel eluting porous carbon–carbon nanoparticle coated, nonpolymeric cobalt–chromium stent: Evaluation in a porcine model. Catheter. Cardiovasc. Interv., 2006;67:698-702.

172. Morice M, Bestehorn H, Carrie D, Macaya C, Aengevareen W, Wijns W, Dubois C, De Winter R, Verheye S, Hoffmann S, Direct stenting of de novo coronary stenoses with tacrolimus-eluting versus carbon-coated carbostents. The randomized JUPITER II trial. EuroIntervention, 2006;2:45-52.

173. Lansky A, Costa R, Mintz G, Tsuchiya Y, Midei M, Cox D, O'Shaughnessy C, Applegate R, Cannon L, Mooney M, Non-polymer-based paclitaxel-coated coronary stents for the treatment of patients with de novo coronary lesions: angiographic follow-up of the DELIVER clinical trial. Circulation, 2004;109:1948-54.

174. Granada JF, Inami S, Aboodi MS, Tellez A, Milewski K, Wallace-Bradley D, Parker S, Rowland S, Nakazawa G, Vorpahl M, Kolodgie FD, Kaluza GL, Leon MB, Virmani R, Development of a Novel Prohealing Stent Designed to Deliver Sirolimus From a Biodegradable Abluminal Matrix. Cir Cardiovas Interv, 2010;3:257-66.

175. Spinke J, Liley M, Guder H, Angermaier L, Knoll W, Molecular recognition at self-assembled monolayers: the construction of multicomponent multilayers. Langmuir, 1993;9:1821-5.

176. Sigal G, Bamdad C, Barberis A, Strominger J, Whitesides G, A self-assembled monolayer for the binding and study of histidine-tagged proteins by surface plasmon resonance. Anal. Chem, 1996;68:490-7.

177. Fujita K, Bunjes N, Nakajima K, Hara M, Sasabe H, Knoll W, Macrodipole interaction of helical peptides in a self-assembled monolayer on gold substrate. Langmuir, 1998;14:6167-72.

178. Houseman B, Gawalt E, Mrksich M, Maleimide-Functionalized Self-Assembled Monolayers for the Preparation of Peptide and Carbohydrate Biochips†. Langmuir, 2003;19:1522-31.

179. Huang E, Zhou F, Studies of surface coverage and orientation of DNA molecules immobilized onto preformed alkanethiol self-assembled monolayers. Langmuir, 2000;16:3272-80.

180. Riepl M, Enander K, Liedberg B, Schäferling M, Kruschina M, Ortigao F, Functionalized surfaces of mixed alkanethiols on gold as a platform for oligonucleotide microarrays. Langmuir, 2002;18:7016-23.

181. Herrwerth S, Rosendahl T, Feng C, Fick J, Eck W, Himmelhaus M, Dahint R, Grunze M, Covalent Coupling of Antibodies to Self-Assembled Monolayers of Carboxy-Functionalized Poly (ethylene glycol): Protein Resistance and Specific Binding of Biomolecules†. Langmuir, 2003;19:1880-7.

182. Kwon Y, Han Z, Karatan E, Mrksich M, Kay B, Antibody arrays prepared by cutinase-mediated immobilization on self-assembled monolayers. Anal. Chem, 2004;76:5713-20.

183. Gawalt E, Avaltroni M, Danahy M, Silverman B, Hanson E, Midwood K, Schwarzbauer J, Schwartz J, Bonding organics to Ti alloys: facilitating human osteoblast attachment and spreading on surgical implant materials. Langmuir, 2003;19:200-4.

184. Adden N, Gamble L, Castner D, Hoffmann A, Gross G, Menzel H, Phosphonic acid monolayers for binding of bioactive molecules to titanium surfaces. Langmuir, 2006;22:8197-204.

185. Mahapatro A, Johnson D, Patel D, Feldman M, Ayon A, Agrawal C, Surface modification of functional self-assembled monolayers on 316L stainless steel via lipase catalysis. Langmuir, 2006;22:901-5.

186. Mahapatro A, Johnson D, Patel D, Feldman M, Ayon A, Agrawal C, Drug delivery from therapeutic self-assembled monolayers (T-SAMs) on 316L stainless steel. Curr Top Med Chem, 2008;8:281-9.

187. Mani G, Johnson D, Marton D, Feldman M, Patel D, Ayon A, Agrawal C, Drug delivery from gold and titanium surfaces using self-assembled monolayers. Biomaterials, 2008;29:4561-73.

188. Tidwell C, Ertel S, Ratner B, Tarasevich B, Atre S, Allara D, Endothelial cell growth and protein adsorption on terminally functionalized, self-assembled monolayers of alkanethiolates on gold. Langmuir, 1997;13:3404-13.

189. Ulman A, Formation and structure of self-assembled monolayers. Chem. Rev, 1996;96:1533-54.

190. Love J, Estroff L, Kriebel J, Nuzzo R, Whitesides G, Self-assembled monolayers of thiolates on metals as a form of nanotechnology. Chem. Rev, 2005;105:1103-70.

191. Gawalt E, Avaltroni M, Koch N, Schwartz J, Self-assembly and bonding of alkanephosphonic acids on the native oxide surface of titanium. Langmuir, 2001;17:5736-8.

192. Helmy R, Fadeev A, Self-assembled monolayers supported on TiO2: comparison of C18H37SiX3 (X= H, Cl, OCH3), C18H37Si (CH3) 2Cl, and C18H37PO (OH) 2. Langmuir, 2002;18:8924-8.

193. Hofer R, Textor M, Spencer N, Alkyl phosphate monolayers, self-assembled from aqueous solution onto metal oxide surfaces. Langmuir, 2001;17:4014-20.

194. Tosatti S, Michel R, Textor M, Spencer N, Self-assembled monolayers of dodecyl and hydroxy-dodecyl phosphates on both smooth and rough titanium and titanium oxide surfaces. Langmuir, 2002;18:3537-48.

195. Zwahlen M, Tosatti S, Textor M, Hähner G, Orientation in methyl-and hydroxyl-terminated self-assembled alkanephosphate monolayers on titanium oxide surfaces investigated with soft X-ray absorption. Langmuir, 2002;18:3957-62.

196. Silverman B, Wieghaus K, Schwartz J, Comparative properties of siloxane vs phosphonate monolayers on a key titanium alloy. Langmuir, 2005;21:225-8.

197. Clair S, Variola F, Kondratenko M, Jedrzejowski P, Nanci A, Rosei F, Perepichka D, Self-assembled monolayer of alkanephosphoric acid on nanotextured Ti. J Chem Phys, 2008;128:144705.

198. Raman A, Dubey M, Gouzman I, Gawalt E, Formation of self-assembled monolayers of alkylphosphonic acid on the native oxide surface of SS316L. Langmuir, 2006;22:6469-72.

199. Kang C, Lee Y, The surface modification of stainless steel and the correlation between the surface properties and protein adsorption. J Mater Sci-Mater Med, 2007;18:1389-98.

200. Puleo D, Biochemical surface modification of Co---Cr---Mo. Biomaterials, 1996;17:217-22.

201. Quiñones R, Gawalt E, Study of the formation of self-assembled monolayers on nitinol. Langmuir, 2007;23:10123-30.

202. Zorn G, Adadi R, Brener R, Yakovlev V, Gotman I, Gutmanas E, Sukenik C, Tailoring the Surface of NiTi Alloy Using PIRAC Nitriding Followed by Anodization and Phosphonate Monolayer Deposition. Chem. Mater, 2008;20:5368-74.

203. De Palma R, Laureyn W, Frederix F, Bonroy K, Pireaux J, Borghs G, Maes G, Formation of dense self-assembled monolayers of (n-decyl) trichlorosilanes on Ta/Ta2O5. Langmuir, 2007;23:443-51.

204. Textor M, Ruiz L, Hofer R, Rossi A, Feldman K, Hähner G, Spencer N, Structural chemistry of self-assembled monolayers of octadecylphosphoric acid on tantalum oxide surfaces. Langmuir, 2000;16:3257-71.

205. Chorny M, Fishbein I, Yellen B, Alferiev I, Bakay M, Ganta S, Adamo R, Amiji M, Friedman G, Levy R, Targeting stents with local delivery of paclitaxel-loaded magnetic nanoparticles using uniform fields. Proceedings of the National Academy of Sciences, 2010;107:8346-51.

206. Polyak B, Fishbein I, Chorny M, Alferiev I, Williams D, Yellen B, Friedman G, Levy RJ, High field gradient targeting of magnetic nanoparticle-loaded endothelial cells to the surfaces of steed stents. Proc. Natl. Acad. Sci. U. S. A., 2008;105:698-703.

207. Wykrzykowska JJ, Onuma Y, Serruys PW, Advances in stent drug delivery: the future is in bioabsorbable stents. Expert Opin. Drug Deliv., 2009;6:113-26.

208. Ormiston J, Serruys P, Bioabsorbable Coronary Stents. Cir Cardiovasc Interv, 2009;2:255-60.

209. Tsuji T; Tamai H; Igaki K H, Y-S, Kosuga K, Hata T, Okada M, Nakamura T, Fujita S, Four-year follow-up of the biodegradable stent (Igaki-Tamai stent). Circ. J., 2004;68:135.

210. Vogt F, Stein A, Rettemeier G, Krott N, Hoffmann R, Dahl J, Bosserhoff AK, Michaeli W, Hanrath P, Weber C, Long-term assessment of a novel biodegradable paclitaxel-eluting coronary polylactide stent. Eur. Heart J., 2004;25:1330-40.

211. Okamura T, Garg S, Gutierrez-Chico JL, Shin E-S, Onuma Y, Garcia-Garcia HM, Rapoza RJ, Sudhir K, Regar E, Serruys PW, In vivo evaluation of stent strut distribution patterns in the bioabsorbable everolimus-eluting device: an OCT ad hoc

analysis of the revision 1.0 and revision 1.1 stent design in the ABSORB clinical trial. EuroIntervention, 2010;5:932-8.

212. Serruys PW, BVS cohort B: device design, 6-month update, and first report of the 12-month results. Proceedings of TCT;, 2010 Sep 21–25;Washington.

213. Ormiston JA, Serruys PW, Regar E, Dudek D, Thuesen L, Webster MWI, Onuma Y, Garcia-Garcia HM, McGreevy R, Veldhof S, A bioabsorbable everolimus-eluting coronary stent system for patients with single de-novo coronary artery lesions (ABSORB): a prospective open-label trial. The Lancet, 2008;371:899-907.

214. Serruys PW, Ormiston JA, Onuma Y, Regar E, Gonzalo N, Garcia-Garcia HM, Nieman K, Bruining N, Dorange C, Miquel-Hébert K, A bioabsorbable everolimus-eluting coronary stent system (ABSORB): 2-year outcomes and results from multiple imaging methods. The Lancet, 2009;373:897-910.

215. Grube E, The REVA tyrosine-derived polycarbonate bioabsorbable stent: final results from the RESORB first-in-man clinical trial and next generation designs. Proceedings of TCT;, 2008 Oct 12–17;Washington.

216. Pollman MJ, Engineering a bioresorbable stent: REVA programme update. EuroIntervention, 2009;5:F54–F7.

217. Abizaid A, The REVA tyrosine-derived polycarbonate bioabsorbable stent: lessons learned and future directions. Proceedings of TCT;, 2009 Sep 21–25; San Francisco.

218. Jabara R, Pendyala, L, Geva, S, Chen, J, Chronos, N, Robinson, K, Novel fully bioabsorbale salicylate-based sirolimuseluting stent. EuroIntervention, 2009;5:F58–F64.

219. Abizaid A, The BTI salycilate-based polyanhydride ester absorbable sirolimus-eluting stent: update from the Whisper study. Proceedings of TCT, 2008 Oct 12–17; Washington.

220. Jabara R, Poly-anhydride based on salicylic acid and adipic acid anhydride. Proceedings of Euro PCR, 2009 May 19–22; Barcelona, Spain.

221. Hermawan H, Dube D, Mantovani D, Developments in metallic biodegradable stents. Acta Biomater., 2010;6:1693-7.

222. Erbel R, Di Mario C, Bartunek J, Bonnier J, de Bruyne B, Eberli FR, Erne P, Haude M, Heublein B, Horrigan M, Ilsley C, Bose D, Koolen J, Luscher TF, Weissman N, Waksman R, Investigators P-A, Temporary scaffolding of coronary arteries with bioabsorbable magnesium stents: a prospective, non-randomised multicentre trial. Lancet, 2007;369:1869-75.

223. Waksman R, Current state of the absorbable metallic (magnesium)stent. EuroIntervention, 2009;5:F94–F8.

224. Kipshidze N, Dangas G, Tsapenko M, Moses J, Leon MB, Kutryk M, Serruys P, Role of the endothelium in modulating neointimal formation - Vasculoprotective approaches to attenuate restenosis after percutaneous coronary interventions. J. Am. Coll. Cardiol., 2004;44:733-9.

225. Consigny PM, Endothelial cell seeding on prosthetic surfaces. J. Long. Term Eff. Med. Implants, 2000;10:79-95.

226. Bailey SR DY, Sprague E, Endothelial seeding: intraprocedural replacement of endothelial cells on endovascular stents. Circulation, 1997;94.

227. Shirota T, Yasui H, Shimokawa H, Matsuda T, Fabrication of endothelial progenitor cell (EPC)-seeded intravascular stent devices and in vitro endothelialization on hybrid vascular tissue. Biomaterials, 2003;24:2295-302.

228. Aoki J, Serruys PW, van Beusekom H, Ong ATL, McFadden EP, Sianos G, van der Giessen WJ, Regar E, de Feyter PJ, Davis HR, Rowland S, Kutryk MJB, Endothelial progenitor cell capture by stents coated with antibody against CD34 - The HEALING-

FIM (healthy endothelial accelerated lining inhibits neointimal growth-first in man) registry. J. Am. Coll. Cardiol., 2005;45:1574-9.

229. Van Belle E, Tio F, Couffinhal T, Maillard L, Passeri J, Isner J, Stent endothelialization: time course, impact of local catheter delivery, feasibility of recombinant protein administration, and response to cytokine expedition. Circulation, 1997;95:438-48.

230. Van Belle E, Tio F, Chen D, Maillard L, Kearney M, Isner J, Passivation of metallic stents after arterial gene transfer of phVEGF165 inhibits thrombus formation and intimal thickening. J. Am. Coll. Cardiol., 1997;29:1371-9.

231. Shantsila E, Watson T, Lip G, Endothelial progenitor cells in cardiovascular disorders. J. Am. Coll. Cardiol., 2007;49:741-52.

232. Tanguay JF, in *58th Annual Meeting of the Canadian-Cardiovascular-Society*, Pulsus Group Inc, Montreal, Canada, 2005, pp. 1025-30.

233. Anis RR, Karsch KR, The future of drug eluting stents. Heart, 2006;92:585-8.

234. Cho HJ, Kim TY, Cho HJ, Park KW, Zhang SY, Kim JH, Kim SH, Hahn JY, Kang HJ, Park YB, Kim HS, The effect of stem cell mobilization by granulocyte-colony stimulating factor on neointimal hyperplasia and endothelial healing after vascular injury with bare-metal versus paclitaxel-eluting stents. J. Am. Coll. Cardiol., 2006;48:366-74.

235. Pelisek J, Fuchs AT, Kuehnl A, Tian W, Kuhlmann MT, Rolland PH, Choukri M, Gaedtke L, Nikol S, C-Type natriuretic peptide for reduction of restenosis: gene transfer is superior over single peptide administration. J. Gene Med., 2006;8:835-44.

236. Patel H, Su S, Patterson C, Nguyen K, A combined strategy to reduce restenosis for vascular tissue engineering applications. Biotechnol. Prog., 2006;22:38-44.

237. Garg S, Duckers HJ, Serruys PW, Endothelial progenitor cell capture stents: will this technology find its niche in contemporary practice? Eur. Heart J., 2010;31:1032-5.

238. Duckers H, Silber S, De Winter R, Heijer P, Rensing B, Rau M, Mudra H, Benit E, Verheye S, Wijns W, Circulating endothelial progenitor cells predict angiographic and intravascular ultrasound outcome following percutaneous coronary interventions in the HEALING-II trial: evaluation of an endothelial progenitor cell capturing stent. EuroIntervention, 2007;3:67-75.

239. Duckers H, Soullie T, Den heijer P, Rensing B, De Winter R, Rau M, Mudra H, Silber S, Benit E, Velheye S, Accelerated vascular repair following percutaneous coronary intervention by capture of endothelial progenitor cells promotes regression of neointimal growth at long term follow-up: final results of the Healing II trial using an endothelial progenitor cell capturing stent (Genous R stent)™. EuroIntervention, 2007;3:350-8.

240. Co M, Tay E, Chi Hang L, Kian K, Low A, Lim J, Use of endothelial progenitor cell capture stent (Genous Bio-Engineered R Stent) during primary percutaneous coronary intervention in acute myocardial infarction: intermediate-to long-term clinical follow-up. Am. Heart J., 2008;155:128-32.

241. Blindt R, Vogt F, Astafieva I, Fach C, Hristov M, Krott N, Seitz B, Kapurniotu A, Kwok C, Dewor M, BosserhofF AK, Bernhagen J, Hanrath P, Hofmann R, Weber C, A novel drug-eluting stent coated with an integrin-binding cyclic Arg-Gly-Asp peptide inhibits neointimal hyperplasia by recruiting endothelial progenitor cells. J. Am. Coll. Cardiol., 2006;47:1786-95.

242. Stefanadis C, Toutouzas K, Stefanadi E, Kolodgie F, Virmani R, Kipshidze N, First experimental application of bevacizumab-eluting PC coated stent for inhibition of vasa vasorum of atherosclerotic plaque: angiographic results in a rabbit atheromatic model. Hellenic J. Cardiol., 2006;47:7-10.

243. Nakazawa G, Granada J, Alviar C, Tellez A, Kaluza G, Guilhermier M, Parker S, Rowland S, Kolodgie F, Leon M, Anti-CD34 antibodies immobilized on the surface of sirolimus-eluting stents enhance stent endothelialization. JACC Interventions, 2010;3:68-75.

244. Flemming RG, Murphy CJ, Abrams GA, Goodman SL, Nealey PF, Effects of synthetic micro- and nano-structured surfaces on cell behavior. Biomaterials, 1999;20:573-88.

245. Norman J, Desai T, Methods for fabrication of nanoscale topography for tissue engineering scaffolds. Ann. Biomed. Eng., 2006;34:89-101.

246. Tseng AA, Notargiacomo A, Nanoscale fabrication by nonconventional approaches. J. Nanosci. Nanotechnol., 2005;5:683-702.

247. Dolatshahi-Pirouz A, Hovgaard MB, Rechendorff K, Chevallier J, Foss M, Besenbacher F, Scaling behavior of the surface roughness of platinum films grown by oblique angle deposition. Phys. Rev. B, 2008;77.

248. Buzea C, Beydaghyan G, Elliott C, Robbie K, Control of power law scaling in the growth of silicon nanocolumn pseudo-regular arrays deposited by glancing angle deposition. Nanotechnology, 2005;16:1986-92.

249. LaFratta CN, Li LJ, Fourkas JT, Soft-lithographic replication of 3D microstructures with closed loops. Proc. Natl. Acad. Sci. U. S. A., 2006;103:8589-94.

250. Pikulin A, Bityurin N, Spatial resolution in polymerization of sample features at nanoscale. Phys. Rev. B, 2007;75.

251. Seunarine K, Meredith DO, Riehle MO, Wilkinson CDW, Gadegaard N, Biodegradable polymer tubes with litho graphically controlled 3D micro- and nanotopography. Microelectron. Eng., 2008;85:1350-4.

252. In HJ, Kumar S, Shao-Horn Y, Barbastathis G, Origami fabrication of nanostructured, three-dimensional devices: Electrochemical capacitors with carbon electrodes. Appl. Phys. Lett., 2006;88.

253. Palmaz JC, Benson A, Sprague EA, Influence of surface topography on endothelialization of intravascular metallic material. J. Vasc. Interv. Radiol., 1999;10:439-44.

254. Fuss C SE, Bailey SR, Palmaz JC. , Surface micro grooves (MG) improve endothelialization rate in vitro and in vivo Am. J. Cardiol., 2001;37(2A):70A.

255. Lu J, Rao M, MacDonald N, Khang D, Webster T, Improved endothelial cell adhesion and proliferation on patterned titanium surfaces with rationally designed, micrometer to nanometer features. Acta Biomater., 2008;4:192-201.

256. Ranjan A, Webster TJ, Increased endothelial cell adhesion and elongation on micron-patterned nano-rough poly(dimethylsiloxane) films. Nanotechnology, 2009;20:305102.

257. Hwang SY, Kwon KW, Jang KJ, Park MC, Lee JS, Suh KY, Adhesion Assays of Endothelial Cells on Nanopatterned Surfaces within a Microfluidic Channel. Anal. Chem., 2010;82:3016-22.

258. Bettinger C, Zhang Z, Gerecht S, Borenstein JT, Langer R, Enhancement of in vitro capillary tube formation by substrate nanotopography. Adv. Mater., 2008;20:99-103.

259. Berry C, McCloy D, Affrossman S, Endothelial cell response to narrow diameter nylon tubes exhibiting internal nanotopography. Current Nanoscience, 2008;4:219-23.

260. Hsu SH, Tang CM, Lin CC, Biocompatibility of poly(epsilon-caprolactone)/poly(ethylene glycol) diblock copolymers with nanophase separation. Biomaterials, 2004;25:5593-601.

261. Dalby MJ, Riehle MO, Johnstone H, Affrossman S, Curtis ASG, In vitro reaction of endothelial cells to polymer demixed nanotopography. Biomaterials, 2002;23:2945-54.

262. Buttiglieri S, Pasqui D, Migliori M, Johnstone H, Affrossman S, Sereni L, Wratten ML, Barbucci R, Tetta C, Camussi G, Endothelization and adherence of leucocytes to nanostructured surfaces. Biomaterials, 2003;24:2731-8.

263. Barbucci R, Pasqui D, Wirsen A, Affrossman S, Curtis A, Tetta C, Micro and nano-structured surfaces. J. Mater. Sci.-Mater. Med., 2003;14:721-5.

264. Kim P, Kim DH, Kim B, Choi SK, Lee SH, Khademhosseini A, Langer R, Suh KY, Fabrication of nanostructures of polyethylene glycol for applications to protein adsorption and cell adhesion. Nanotechnology, 2005;16:2420-6.

265. Zawislak JD, Kolasinski KW, Helmke BP, Development of endothelial cells on pillar-covered silicon. Physica Status Solidi a-Applications and Materials Science, 2009;206:1356-60.

266. Choudhary S, Berhe M, Haberstroh KM, Webster TJ, Increased endothelial and vascular smooth muscle cell adhesion on nanostructured titanium and CoCrMo. Int. J. Nanomedicine, 2006;1:41-9.

267. Choudhary S, Haberstroh KM, Webster TJ, Enhanced functions of vascular cells on nanostructured Ti for improved stent applications. Tissue Eng., 2007;13:1421-30.

268. Khang D, Lu J, Yao C, Haberstroh KM, Webster TJ, The role of nanometer and sub-micron surface features on vascular and bone cell adhesion on titanium. Biomaterials, 2008;29:970-83.

269. Peng L, Eltgroth ML, LaTempa TJ, Grimes CA, Desai TA, The effect of TiO2 nanotubes on endothelial function and smooth muscle proliferation. Biomaterials, 2009;30:1268-72.

270. Samaroo HD, Lu J, Webster TJ, Enhanced endothelial cell density on NiTi surfaces with sub-macron to nanometer roughness. Int. J. Nanomedicine, 2008;3:75-82.

271. Carpenter J, Khang D, Webster TJ, Nanometer polymer surface features: the influence on surface energy, protein adsorption and endothelial cell adhesion. Nanotechnology, 2008;19.

272. Serrano MC, Portoles MT, Vallet-Regi M, Izquierdo I, Galletti L, Comas JV, Pagani R, Vascular endothelial and smooth muscle cell culture on NaOH-treated poly (epsilon-caprolactone) films: A preliminary study for vascular graft development. Macromol. Biosci., 2005;5:415-23.

273. Miller DC, Thapa A, Haberstroh KM, Webster TJ, Endothelial and vascular smooth muscle cell function on poly(lactic-co-glycolic acid) with nano-structured surface features. Biomaterials, 2004;25:53-61.

274. Lord MS, Cousins BG, Doherty PJ, Whitelock JM, Simmons A, Williams RL, Milthorpe BK, The effect of silica nanoparticulate coatings on serum protein adsorption and cellular response. Biomaterials, 2006;27:4856-62.

275. Sarkar S, Dadhania M, Rourke P, Desai TA, Wong JY, Vascular tissue engineering: microtextured scaffold templates to control organization of vascular smooth muscle cells and extracellular matrix. Acta Biomater., 2005;1:93-100.

276. Glawe JD, Hill JB, Mills DK, McShane MJ, Influence of channel width on alignment of smooth muscle cells by high-aspect-ratio microfabricated elastomeric cell culture scaffolds. J. Biomed. Mater. Res. Part A, 2005;75A:106-14.

277. Houtchens GR, Foster MD, Desai TA, Morgan EF, Wong JY, Combined effects of microtopography and cyclic strain on vascular smooth muscle cell orientation. J. Biomech., 2008;41:762-9.

278.   Yim EKF, Reano RM, Pang SW, Yee AF, Chen CS, Leong KW, Nanopattern-induced changes in morphology and motility of smooth muscle cells. Biomaterials, 2005;26:5405-13.
279.   Richert L, Vetrone F, Yi JH, Zalzal SF, Wuest JD, Rosei F, Nanci A, Surface nanopatterning to control cell growth. Adv. Mater., 2008;20:1488-92.
280.   Nguyen KT, Shukla KP, Moctezuma M, Tang LP, Cellular and molecular responses of smooth muscle cells to surface nanotopography. J. Nanosci. Nanotechnol., 2007;7:2823-32.
281.   Gao JM, Niklason L, Langer R, Surface hydrolysis of poly(glycolic acid) meshes increases the seeding density of vascular smooth muscle cells. J. Biomed. Mater. Res., 1998;42:417-24.
282.   Thapa A, Miller DC, Webster TJ, Haberstroh KM, Nano-structured polymers enhance bladder smooth muscle cell function. Biomaterials, 2003;24:2915-26.
283.   Walboomers XF, Croes HJE, Ginsel LA, Jansen JA, Growth behavior of fibroblasts on microgrooved polystyrene. Biomaterials, 1998;19:1861-8.
284.   Walboomers XF, Croes HJE, Ginsel LA, Jansen JA, Contact guidance of rat fibroblasts on various implant materials. J. Biomed. Mater. Res., 1999;47:204-12.
285.   Walboomers XF, Monaghan W, Curtis ASG, Jansen JA, Attachment of fibroblasts on smooth and microgrooved polystyrene. J. Biomed. Mater. Res., 1999;46:212-20.
286.   Walboomers XF, Ginsel LA, Jansen JA, Early spreading events of fibroblasts on microgrooved substrates. J. Biomed. Mater. Res., 2000;51:529-34.
287.   Meyle J, Gultig K, Nisch W, Variation in contact guidance by human-cells on a microstructured surface. J. Biomed. Mater. Res., 1995;29:81-8.
288.   Lee SW, Kim SY, Rhyu IC, Chung WY, Leesungbok R, Lee KW, Influence of microgroove dimension on cell behavior of human gingival fibroblasts cultured on titanium substrata. Clin. Oral Implants Res., 2009;20:56-66.
289.   Chou LS, Firth JD, Uitto VJ, Brunette DM, Substratum surface - topography alters cell-shape and regulates fribronectin messenger-RNA level, messenger-RNA stability, secretion and assembly in human fibroblasts J. Cell Sci., 1995;108:1563-73.
290.   Biela SA, Su Y, Spatz JP, Kemkemer R, Different sensitivity of human endothelial cells, smooth muscle cells and fibroblasts to topography in the nano-micro range. Acta Biomater., 2009;5:2460-6.
291.   Loesberg WA, te Riet J, van Delft F, Schon P, Figdor CG, Speller S, van Loon J, Walboomers XF, Jansen JA, The threshold at which substrate nanogroove dimensions may influence fibroblast alignment and adhesion. Biomaterials, 2007;28:3944-51.
292.   Sun F, Casse D, van Kan JA, Ge RW, Watt F, Geometric control of fibroblast growth on proton beam-micromachined scaffolds. Tissue Eng., 2004;10:267-72.
293.   Berry CC, Dalby MJ, McCloy D, Affrossman S, The fibroblast response to tubes exhibiting internal nanotopography. Biomaterials, 2005;26:4985-92.
294.   Dalby MJ, Riehle MO, Johnstone H, Affrossman S, Curtis ASG, Investigating the limits of filopodial sensing: a brief report using SEM to image the interaction between 10 nm high nano-topography and fibroblast filopodia. Cell Biol. Int., 2004;28:229-36.
295.   Dalby MJ, Riehle MO, Johnstone HJH, Affrossman S, Curtis ASG, Nonadhesive nanotopography: Fibroblast response to poly(n-butyl methacrylate)-poly(styrene) demixed surface features. J. Biomed. Mater. Res. Part A, 2003;67A:1025-32.
296.   Dalby MJ, Riehle MO, Johnstone HJH, Affrossman S, Curtis ASG, Polymer-demixed nanotopography: Control of fibroblast spreading and proliferation. Tissue Eng., 2002;8:1099-108.

297. Dalby MJ, Giannaras D, Riehle MO, Gadegaard N, Affrossman S, Curtis ASG, Rapid fibroblast adhesion to 27 nm high polymer demixed nano-topography. Biomaterials, 2004;25:77-83.

298. Dalby MJ, Gadegaard N, Riehle MO, Wilkinson CDW, Curtis ASG, Investigating filopodia sensing using arrays of defined nano-pits down to 35 nm diameter in size. Int. J. Biochem. Cell Biol., 2004;36:2005-15.

299. Dalby MJ, Gadegaard N, Wilkinson CDW, The response of fibroblasts to hexagonal nanotopography fabricated by electron beam lithography. J. Biomed. Mater. Res. Part A, 2008;84A:973-9.

300. Green AM, Jansen JA, Vanderwaerden J, Vonrecum AF, Fibroblast response to microtextured silicone surfaces: texture orientation into or out of the surface. J. Biomed. Mater. Res., 1994;28:647-53.

301. Milner KR, Siedlecki CA, Submicron poly(L-lactic acid) pillars affect fibroblast adhesion and proliferation. J. Biomed. Mater. Res. Part A, 2007;82A:80-91.

302. Milner KR, Siedlecki CA, Fibroblast response is enhanced by poly(L-lactic acid) nanotopography edge density and proximity. Int. J. Nanomedicine, 2007;2:201-11.

303. Hunt JA, Williams RL, Tavakoli SM, Riches ST, Laser surface modification of polymers to improve biocompatibility. J. Mater. Sci.-Mater. Med., 1995;6:813-7.

304. Dalby MJ, Berry CC, Riehle MO, Sutherland DS, Agheli H, Curtis ASG, Attempted endocytosis of nano-environment produced by colloidal lithography by human fibroblasts. Exp. Cell Res., 2004;295:387-94.

305. Choi CH, Hagvall SH, Wu BM, Dunn JCY, Beygui RE, Kim CJ, Cell interaction with three-dimensional sharp-tip nanotopography. Biomaterials, 2007;28:1672-9.

306. Choi CH, Heydarkhan-Hagvall S, Wu BM, Dunn JCY, Beygui RE, Kim CJ, Cell growth as a sheet on three-dimensional sharp-tip nanostructures. J. Biomed. Mater. Res. Part A, 2009;89A:804-17.

307. Dalby MJ, Riehle MO, Sutherland DS, Agheli H, Curtis ASG, Use of nanotopography to study mechanotransduction in fibroblasts - methods and perspectives. Eur. J. Cell Biol., 2004;83:159-69.

308. Dalby MJ, Biggs MJP, Gadegaard N, Kalna G, Wilkinson CDW, Curtis ASG, Nanotopographical stimulation of mechanotransduction and changes in interphase centromere positioning. J. Cell. Biochem., 2007;100:326-38.

309. Vance RJ, Miller DC, Thapa A, Haberstroh KM, Webster TJ, Decreased fibroblast cell density on chemically degraded poly-lactic-co-glycolic acid, polyurethane, and polycaprolactone. Biomaterials, 2004;25:2095-103.

310. Cousins BG, Doherty PJ, Williams RL, Fink J, Garvey MJ, The effect of silica nanoparticulate coatings on cellular response. J. Mater. Sci.-Mater. Med., 2004;15:355-9.

311. Dalby M, Riehle M, Johnstone H, Affrossman S, Curtis A, Polymer-demixed nanotopography: control of fibroblast spreading and proliferation. Tissue Eng., 2002;8:1099-108.